Finite size effects of itinerant electron systems on Curie temperature

Peters, L.

Award date:
2010

Finite size effects of weak itinerant electron systems on Curie temperature

Author: Lars Peters
Supervisors: Dr. Andrei Kirilyuk and
Prof. Mikhail Katsnelson
Coordinator: Prof. Paul Koenraad

Date: October 2010

Summary

Self consistent renormalization theory of itinerant magnets is used to calculate the Curie temperature of a cluster system. Here a cluster is an almost spherical particle having microscopic (atomic) variations of the surface. A cluster system is then a collection of clusters of the same size, but different in this surface roughness. In these clusters the electrons responsible for the magnetic properties are assumed to be itinerant. The size range considered here are clusters of approximately 100 atoms and larger.
Random matrix theory is used for the calculation of the energy level distribution in a cluster system. It appears that due to the atomic surface irregularities energy level repulsion occurs. The effect of this is that the spin density fluctuations are suppressed leading to an increase in the Curie temperature compared to the bulk. This unexpected result actually shows an increase towards smaller cluster sizes.

Table of contents

Introduction

This introduction serves three purposes. (I) It gives a description and motivation for the research done. (II) The system under investigation is described in detail. (III) The organization of the report is given.

Motivation

The regime of the isolated atom and the bulk are well established, meaning that the physical and chemical properties of them are well known [1]. However, the regime in between (figure I), corresponding to so called clusters is quite unfamiliar. In general a cluster is defined as a particle containing more than 2 atoms. Thus, in figure I the two middle pictures correspond to clusters. From a fundamental point of view the study of this regime is crucial and interesting in the understanding of how physical and chemical properties develop from the atomic to the bulk regime. It appears that clusters possess interesting properties different from that of the atom and bulk [1,2,3]. For example by changing the size certain properties can be controlled such as magnetic and catalytic properties.

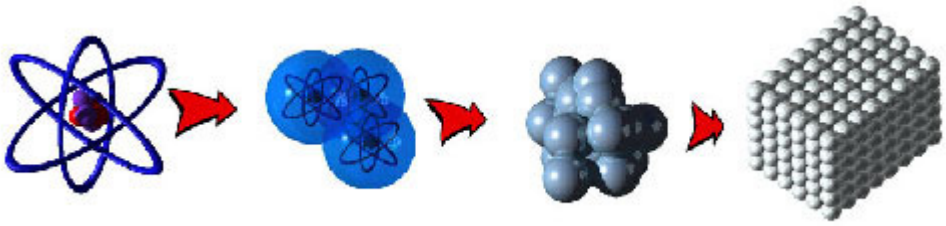

Figure I: going from an isolated atom to a small cluster, to a larger cluster and finally to bulk [4].

Research in cluster physics is not only interesting from a fundamental point of view. A deep understanding of the electronic and ionic structure is crucial for practical applications in catalysis, nano-structures, development of new materials, the design of drugs etc. [3].

Further, the next step of miniaturizing devices will include devices in the cluster size regime. An example is the downscaling of the storage volume of a bit in computers. By downscaling the storage volume of a bit, a magnetic moment in specific direction (up or down), it is important to know how the properties of this volume element change. Imagine that for smaller volume sizes the Curie temperature of the volume element drops below room temperature. Then cooling systems are necessary in your computer, which should run day and night to keep your data safe. Whatever the consequence of down scaling will be, it is important to understand the physical principles behind it. Afterwards, when this is understood, technical tricks can be developed to overcome the problems.

In this report the focus will be on the magnetic properties, in particular the Curie temperature, of clusters. The question however, is from which limit a cluster should be approached: atomic, building a cluster atom-by-atom, or reducing size from the bulk. With other words large enough cluster sizes are investigated so that the usual analytical solid state methods are valid. In the following paragraph a precise description of the system under investigation is given.

System under investigation

For small particles measurements are mostly done on a collection of similar, but not identical particles [2]. This collection of particles contains a certain shape and size distribution. That the particles are not identical is caused by the production technique. For a possible production technique the reader is referred to [5].
In this report a collection of small spherical particles of the same size, but with different atomic surface irregularities will be considered. The size regime of the particles under consideration is roughly more than 100 atoms per particle. In figure II an example of a cluster is given. The surface roughness due to the atoms can be clearly seen.

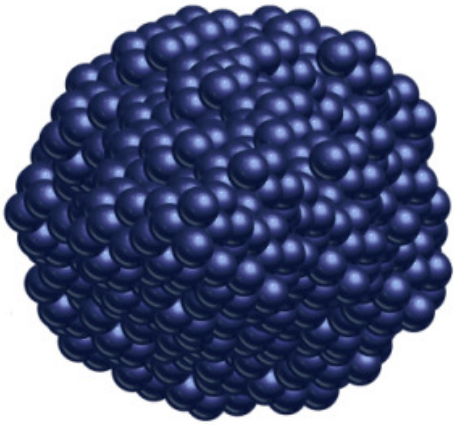

Figure II: schematic picture of an almost spherical cluster with atomic surface irregularities.

The magnetic properties of these small particles are assumed to be caused by the spins of itinerant (delocalized) electrons. Transition metals and some weakly ferromagnetic materials ($ZrZn_2$ and Sc_3In) are examples of systems where itinerant electrons are responsible for the magnetic properties.
Further, some other general assumptions are made, such as: (I) The individual small particles are isolated meaning that they do not interact with each other. (II) There are no external fields such as electric and magnetic fields. (III) Spin-orbit coupling is neglected so that spin is a good quantum number.
Small particles are also called clusters in literature. In this report the word cluster will refer to a single small particle and a cluster system to a collection of small particles differing in shape, but with the same size.

Organization of report

The goal of this report is to investigate how the Curie temperature of a cluster system depends on the cluster size and compare it with the bulk limit. To approach this problem basic theory of magnetism is needed. Therefore, in the first chapter the main developments in theory of magnetism are discussed. This should give an idea of the complexity and diversity of magnetic systems. It should also give a feeling for the difference between localized and itinerant electron magnetism. At the end of this chapter the Hubbard model is treated on which the rest of the theory in this report is based.
Chapter 2 treats the most important steps of the itinerant electron magnetism theory for bulk materials. These developments are based on the Hubbard model. Further, this

chapter shows the importance of taking electron-electron interactions in a self consistent manner into account.
The third and last chapter is devoted to the calculation of the Curie temperature of cluster systems. In this chapter first the general idea for this calculation is discussed. Then various approaches to the theory of cluster systems will be discussed. With the help of this general theory, it is then possible to calculate key quantities required for the calculation of the Curie temperature. At the end all this theory and calculated quantities will come together to show what happens with the Curie temperature of a cluster system as compared to the bulk limit.

Chapter 1: Introduction to models of magnetism

In this chapter a general introduction to various theoretical models describing magnetism will be given. This variety is actually very large owing to the multitude of different types of magnetic materials and magnetic properties. The aim of this chapter is thus to create an overview of these models and to relate them to specific kinds of magnetic materials. The consideration is started with the simplest Hubbard model that includes nearest neighbor hopping only. It will be demonstrated that already such a simple model may provide a decent description of rather different kinds of magnetic materials. In particular, anti-ferromagnetism of insulators and ferro- and antiferromagnetism of some itinerant materials can be understood. For the understanding of the properties of other possible types of magnetic materials somewhat modified versions of the Hubbard model can be used.

However, before going into the details of the quantum mechanical Hubbard model and extensions of it, first the most important classical concepts are briefly discussed.

1.1 Classical models

It was with the model of Langevin where the modern theory of magnetism started [6]. He introduced the concept of local magnetic moments of the same size and calculated how a non-interacting collection of these moments reacted on an externally applied magnetic field. The reaction of this system appeared to be described by the well known Curie law:

$$\chi = \frac{C}{T}, \tag{1.1}$$

where χ is the static magnetic susceptibility, T is the temperature and C is a constant. For small external magnetic fields this static magnetic susceptibility describes how the system responds to an external magnetic field H:

$$\vec{M} = \chi \cdot \vec{H}, \tag{1.2}$$

where $\vec{M}$ is the magnetization of the system. For anisotropic media the χ in the expression (1.2) should be interpreted as a tensor.

Weiss came with an extension of the Langevin theory by assuming a finite interaction between these localized magnetic moments. He approximated this interaction by a mean molecular field proportional to the average magnetization of the system. With this improvement, ferromagnetism could be described and the response of the system to an externally applied magnetic field at high temperatures was shown to be described by the so called Curie-Weiss law:

$$\chi = \frac{C}{T - T_c}, \tag{1.3}$$

where T_c is the Curie temperature of the system. Further, Weiss could also calculate the spontaneous magnetization as function of temperature. This is depicted together with the Curie-Weiss law in figure 1.1.1.

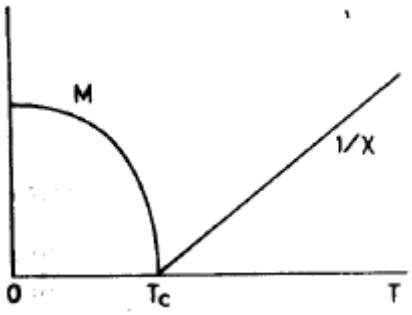

Figure 1.1.1: schematic picture of magnetization and static magnetic susceptibility as function of temperature predicted by Weiss [7].

Although Langevin-Weiss theory was quite successful in describing the main properties of ferromagnets both below and above the Curie temperature, there were two difficulties. First, the existence of these localized magnetic moments of fixed size was impossible to explain. Second, the enormous magnitude of the mean molecular field of about 1000 Tesla introduced by Weiss could not be explained. It was not before the development of quantum mechanics that these problems could be solved [5,7]. Since the advent of quantum mechanics, however, a large variety of different models have been developed to understand the magnetic properties of different kinds of magnetic materials. A good approach to create an overview of these models and the kind of magnetic materials they describe is to look at the so-called Hubbard model [8,9]. We start by considering this model including nearest neighbor interactions only and then look at different modifications of it.

1.2 Hubbard model

In this paragraph the Hubbard model is discussed, starting with nearest neighbor hopping only. The goal of this consideration will be to draw a phase diagram able to give a classification of all encountered magnetic materials. The corresponding modifications of this simple Hubbard model required to improve the description at various points of this phase diagram will also be discussed.

1.2.1 General introduction

The Hubbard model with nearest neighbor hopping only is actually a simplified version of what is usually called the Hubbard model. The Hamiltonian of the Hubbard model is given by:

$$H = \sum_{j,l}\sum_{\sigma} t_{jl} c^{*}_{j\sigma} c_{l\sigma} + U \sum_{j} n_{j\uparrow} n_{j\downarrow} , \qquad (1.4)$$

where j and l indicate atomic sites, t_{jl} is the transfer integral between the Wannier orbital at site j and the same Wannier orbital at site l, $c_{l\sigma}$ is the annihilation operator of the Wannier state at site l, U is the on site interaction energy when two electrons occupy the same site and $n_{j\uparrow}$ is the spin up occupation number operator working on site j. What a Wannier state is will be explained later on. From equation (1.4) it can be seen that the first term is just the tight binding model [10,11] where the electrons occupy a modified atomic orbital localized at an atomic site and can hop from site to site due to the wave function overlap. To be more precise, only one atomic orbital is available at each atomic site (spin degeneracy not taken into account). With other words only one band is formed due to the overlap of these orbitals between different sites.
By using the Fourier transform the tight binding term H_{band} of (1.4) can be rewritten in k-space as

$$H_{band} = \sum_{k}\sum_{\sigma} \varepsilon(\vec{k}) b^{*}_{k\sigma} b_{k\sigma} \,, \tag{1.5}$$

where $b_{k\sigma}$ is now the annihilation operator of the well known Bloch state with wave vector k and spin σ, and $\varepsilon(\vec{k})$ is the dispersion relation of the electrons. It is now clear that the Wannier state is the Fourier transform of the Bloch state.
In the tight binding model interactions between electrons are not considered at all. The Hubbard model includes on-site interactions between the electrons which stems from the Coulomb repulsion. This on-site interaction means that electrons only 'see' each other when they are on the same atomic site. Though it sounds oversimplified, this could be a good approximation in many situations as it will be demonstrated in the next chapter.
Due to this interaction term, there will be a competition between the transfer integral which is a function of distance and angles between the different sites, and the on-site repulsion which is not. This transfer integral, or tight binding term, wants to delocalize the electrons into itinerant Bloch states, such delocalization leading to a metallic behavior. On the other hand the on-site repulsion favors the localization of electrons on the sites, which opposes the metallic behavior.

In the following the consequences of these two opposing tendencies will be discussed. The Hamiltonian of the Hubbard model with nearest neighbor hopping only can be rewritten as:

$$H = H_{band} + H_{Coulomb} = \varepsilon \sum_{j}\sum_{\sigma} n_{j\sigma} - t \sum_{\langle i,j \rangle} \left(c^{*}_{j\sigma} c_{i\sigma} + c^{*}_{i\sigma} c_{j\sigma} \right) + U \sum_{j} n_{j\uparrow} n_{j\downarrow} \,, \tag{1.6}$$

where ε is the energy that the electron obtains from the atomic potential, t is the transfer integral between two Wannier states that represent nearest neighbors, and $\langle i, j \rangle$ indicates that the sum is taken only over nearest neighbor sites. In equation (1.6) the first term merely gives a constant factor.
It can be shown that the zero temperature behavior of this model is determined by the relative interaction strength U/t and the electron density $n = N/L$, where N is the total number of electrons and L the number of lattice sites. Thus, in general $0 \le n \le 2$ and n=1

corresponds to the case of equal number of electrons and atomic sites. This situation of $n=1$ is also called half filling, because half of the available states is occupied. In the beginning of this chapter the phase diagram of the Hubbard model was mentioned. By phase diagram it is meant that as a function of U/t and n, different magnetic and metallic behavior of the system can be found. Now, the phase diagram following from (1.6) will be discussed. In addition, whenever necessary, we describe the required modifications and improvements. In general, the discussion of the conducting properties is followed by the treatment of the magnetic ones.

1.2.2 Metal or insulator?

By using equation (1.6) for half filling ($n=1$) of the band, a metal-insulator transition can be predicted at a certain critical U_{cr}/t value. That such a transition should exist is clear from the following. Imagine one starts with $U=0$, then the ground state is given by the metallic Fermi sea,

$$\left|FS\right\rangle = \prod_{\vec{k}}^{\varepsilon_{\vec{k}}<\varepsilon} c^{*}_{\vec{k}\sigma} c_{\vec{k}\sigma} \left|0\right\rangle , \tag{1.7}$$

where $\left|0\right\rangle$ is the vacuum state and $\varepsilon_{\vec{k}}$ is the dispersion of the electrons. This $\varepsilon_{\vec{k}}$ is found by using the Fourier transform to rewrite the first two terms of (1.6) resulting in

$$H_{band} = \sum_{k}\sum_{\sigma} \varepsilon_{\vec{k}} c^{*}_{\vec{k}\sigma} c_{\vec{k}\sigma} . \tag{1.8}$$

It is clear from (1.7) that the electrons are uncorrelated, which means that the occupation of an orbital by a spin-up electron is independent from its occupation by a spin-down electron. Thus, the probability that a site is occupied by a spin-up electron is a half which is also equal to the probability that a site is occupied by a spin-down electron. The probability to find a double occupied site is therefore 1/4.
Turning the interaction on ($U>0$) and assuming that the ground state is given by (1.7), one derives the following expectation energy of the Coulomb energy:

$$\left\langle FS\middle|H_{Coulomb}\middle|FS\right\rangle = \frac{LU}{4} . \tag{1.9}$$

The band energy is determined by the occupied part of the band and can be written as

$$\left\langle FS\middle|H_{band}\middle|FS\right\rangle = L\left(\varepsilon - \alpha \cdot t\right). \tag{1.10}$$

Here the term between the brackets is the average band energy, where α is of the other of unity and depends on the band shape. For the uncorrelated ground state (1.7), the total energy density can be written as

$$\frac{1}{L}\langle FS|H|FS\rangle = \varepsilon - \alpha \cdot t + \frac{U}{4} \quad . \tag{1.11}$$

From this total energy expression it can be easily understood how a metal insulator transition appears. Indeed, at *U=0* the ground state is given by (1.7) where the electrons are uncorrelated. Thus on average 1/4 of the sites are empty, 1/4 of the sites are doubly occupied and the rest is singly occupied. This means that there are a lot of charge fluctuations. Therefore, the system is a metal. However, by increasing *U/t* one comes to a point where it becomes more favorable for electrons that each site is occupied by a single electron. With other words the total energy of the Fermi sea given by (1.11) exceeds the energy of an assembly of *L* neutral atoms. Therefore above some critical value of *U/t* the electrons become localized which means that the system has become an insulator. Such an insulator where the localization of the electrons is caused by the interaction between them is called a Mott-insulator. There are also insulators where the insulating properties are caused by the long range magnetic order itself. These kinds of insulators have different behavior compared to the Mott-insulators, but they will not be discussed here.

This is actually only a qualitative argument for the existence of a metal insulator transition at half filling. For a more quantitative derivation the reader is referred to [9]. Further, it was assumed that *n=1*. In the following there will be shortly discussed what happens for situations where $n \neq 1$. For metallic behavior in the *n=1* case charge fluctuations are present. This means that there are both empty and doubly occupied sites. The tendency to doubly occupy a site is opposed by the on site interaction term. Therefore, in case of *n=1* only for low enough values of *U/t* metallic behavior will occur as explained above. However, for the $n \neq 1$ case the situation is different. This is caused by the fact that not all the sites are occupied (for *n<1*) or there are already doubly occupied sites present (*n>1*). Thus, for *n<1* there are always electrons that can move unhindered from an occupied state to an empty state even when *U>>t*. For the *n>1* case there is a similar situation; there are always electrons moving unhindered from a double occupied state to a single occupied state even for *U>>t*. With unhindered is meant without increasing the total energy of the system. Concluding, away from half filling the behavior is metallic even for large *U/t*.
This finalizes the discussion of the conducting properties of systems described by the Hamiltonian (1.6). In the following the magnetic properties will be discussed as function of *n* and *U/t* for the Hubbard model with nearest neighbor hopping.

1.2.3 Magnetic properties

Let us start with the discussion of the magnetic properties at *n=1* and *U>>t*. For *U>>t* equation (1.6) can be approximated to the order of t^2/U as the well known anti-ferromagnetic Heisenberg exchange model

$$H = J \sum_{\langle i,j \rangle} \vec{S}_i \cdot \vec{S}_j \,, \tag{1.12}$$

where $J=4t^2/U$. For a derivation of (1.12) see [9]. Thus the system of hopping electrons with on-site interaction only can be approximated by a system of localized spins coupled to their nearest neighbors by the exchange constant J. From (1.12) it can be seen that $J>0$ and that therefore anti-parallel nearest neighbor spins are preferred meaning that for $n=1$ and $U>>t$ the system is anti-ferromagnetic. It was already discussed above that for $U>>t$ the system is a Mott insulator. Thus Mott insulators are anti-ferromagnets according to (1.12). This is however not the complete story. First of all, most anti-ferromagnetic Mott insulators are transition metal compounds. In these systems the *d*-electron bearing cations are separated by large anions. Therefore the direct hopping between the *d*-orbitals is not very probable. Anderson solved this problem by taking covalent mixing into account between the orbitals of the cation and anion [9]. He showed that this anion mediated exchange better known as superexchange favors anti-ferromagnetic coupling in most cases.

Another problem was that not all Mott insulators appeared to be anti-ferromagnetic; some are ferromagnetic. This problem can in principal be solved by using an extended Hubbard model. "Extended" means that besides on site interaction (U), also Coulomb repulsion between nearest neighbor sites (V), direct exchange (F), Coulomb assisted hopping of both one electron (X) and two electrons (Y) at a time are taken into account. In the extended Hubbard model the effective exchange coupling is given by $J_{eff} \sim -F + \frac{(t-X)^2}{U-V}$. This means that for certain combinations of the parameters ferromagnetic coupling will be favorable.

Besides these extended Hubbard terms for certain combinations of parameters, there is orbital degeneracy which favors ferromagnetism. It actually depends on the material under investigation, which of these two mechanisms is dominating. They could also contribute equally. The important thing to remember is that equation (1.6) does not cover the whole story of Mott insulators and that in some situations considerable modifications are required.

For the case of $n \neq 1$ as well as for $n=1$ in the intermediate and small U/t regime the story is more complicated. Namely, it appears to be difficult to indicate a common mechanism for all the different types of magnetic systems. For example there is a group where the magnetic ordering is mostly band structure related. Referring to equation (1.6), this means that the competition between the second and third term determines the magnetic ordering. This second term strongly depends on lattice structure.

Besides these band structure related magnetic systems, there could be other types of magnetic systems where for example orbital degeneracy or extended Hubbard terms are important for the determination of the magnetic ordering.

In the following a cubic lattice structure will be discussed by using equation (1.6). This will actually lead to the conclusion that this lattice structure is unfavorable for ferromagnetism. The discussion is then extended to different lattice structures. It will appear that a certain group of them does favor ferromagnetism. Further, the effect of some modifications to (1.6) will be discussed.

A schematic phase diagram of a cubic lattice at T=0K is depicted in figure 1.2.3.1.

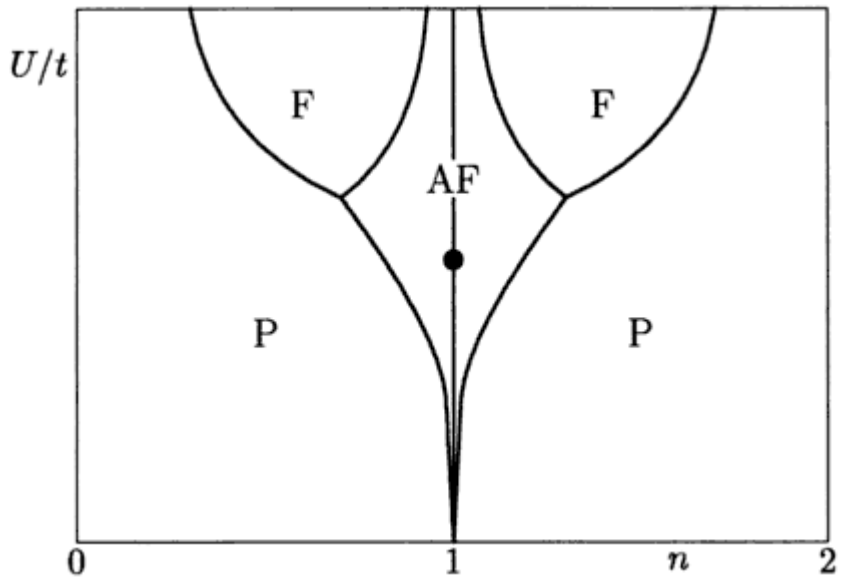

Figure 1.2.3.1: schematic overview of mean field phase diagram of cubic lattice Hubbard model with nearest neighbor hopping only at *T=0K*. The F represents the ferromagnetic phase, AF the anti-ferromagnetic phase and the P the paramagnetic phase. *U/t* is the relative interaction strength and *n* is the electron density. The dot is where the Mott transition occurs [9].

In this figure P stands for paramagnetic phase, F for ferromagnetic phase and AF for anti-ferromagnetic phase. It is assumed here that ferro –and anti-ferromagnetic are the only possible magnetic orderings. In the whole regime except for $n=1$ and $U>U_{cr}$ the magnetic ordering is found by using a mean field approximation. This means that the transition from paramagnetic to ferromagnetic is determined by the well known Stoner criterion (chapter 2), $I\rho(E_F)>1$ with $\rho(E_F)$ the density of states near the Fermi level and I proportional to U. For the transition from paramagnetic to anti-ferromagnetic a similar kind of criterion can be derived. More details of this phase diagram, for example the meaning of the black dot, can be found in [9].
From figure 1.2.3.1 it seems that ferromagnetism is stable in a large part of the phase diagram. However, it is well known that in the mean field theory spin density fluctuations are neglected and that by taking these into account the ferromagnetic phase in figure 1.2.3.1 would shrink. Intensive research has indicated that ferromagnetism in the model of (1.6) is in fact an artifact of the mean field theory. Indeed, by using more sophisticated treatments, which take spin density fluctuations into account, it appears that the ferromagnetic phase shrinks towards a small range of n and large values of U/t. Numerical calculations and for example the variational approach which includes correlation effects by Gutzwiller projecting the mean field states have shown this [9]. Normally the variational approach verifies whether the fully polarized state is stable against a spin flip. In this way it can be found in which part of the phase diagram the fully polarized state is stable. The size of this area is thus an indication of the tendency of the system to be ferromagnetic.
Besides the cubic lattice structure, other structures were investigated by numerical calculations and the variational approach. The outcome was that bipartite lattice structures like the cubic and square lattices are not favorable for ferromagnetism. This

means that for bipartite lattices ferromagnetism was observed only for very large values of U/t and in a narrow range of n. However, non-bipartite lattice structures like the fcc show a strong tendency towards ferromagnetism. Namely, ferromagnetism for a fcc lattice structure is already observed for $U \sim t$. This increased tendency towards ferromagnetism for non-bipartite lattice structures is caused by the asymmetry in the band. The fcc lattice has for example a large peak in the density of states at the bottom of the band. For small n (Fermi level near peak) this is favorable for ferromagnetism, because the on site interaction can be significantly lowered by only increasing marginally the band energy by putting electrons into higher energy states above the Fermi level.
Bipartite lattices have symmetric band structures and therefore symmetric density of states. Even if there is a peak at the center of the band or two peaks at symmetric positions around the center, this is less favorable for ferromagnetism than one peak at one of the band edges [9], even though the peak itself is more favorable for ferromagnetism compared to the situation without a peak. This can be understood by the Stoner criterion given above.
Thus an asymmetric band is favorable for ferromagnetism. Bipartite lattices have symmetric bands within the model of (1.6). It must be mentioned that the term bipartite is not only referring to lattice structure or geometry. For example by fine tuning the band term adding next-nearest neighbor hopping or even further hopping can result in non-bipartite lattices and therefore asymmetric bands. With nearest neighbor hopping only the square lattice is for example bipartite resulting in a symmetric band. Adding next nearest neighbor hopping makes the lattice non-bipartite and therefore results in an asymmetric band.
Whether the band structure is the main mechanism of ferromagnetism in the material under investigation has to be checked. For example orbital degeneracy and the extended Hubbard terms discussed above could also be favorable for ferromagnetism.
There are materials of which there is well known that the magnetic properties are determined by band structure. For example the weak itinerant ferromagnets $ZrZn_2$ and Sc_3In. Weakly ferromagnetic means that the Stoner criterion is only marginally satisfied. Thus $I\rho(E_F)-1$ is a small quantity and therefore these systems have low Curie temperatures (Chapter 2). Although these materials have a peak in the density of states near the Fermi level, the Stoner criterion is barely satisfied because of the weak interaction between the electrons (small I).
When it is clear that the magnetic ordering is a band structure related phenomenon, it is natural to use the Hubbard model (equation (1.4)). The first term is then just the tight-binding model for which many techniques are developed to calculate it [7]. In principle this is what Moriya did to explain the properties of the weakly ferromagnetic materials discussed above [7]. This approach will be discussed in details in the next chapter.
This theory of Moriya gives good results for weakly itinerant (anti-)ferromagnetic systems where the band structure is mainly responsible for the ferromagnetic properties. However, for materials where $I\rho(E_F)-1$ is a large quantity it is known that the theory of Moriya fails [7]. A theory for these materials still has to be developed. At the end of this chapter some words will be dedicated to this.

In the limit of $U>>t$ and for $n \neq 1$, theory is well developed. For this regime it can be shown that equation (1.6) can be approximated to order t^2/U as the so called t-J model

$$H = -t\sum_{\langle i,j\rangle}\left[(1-n_{i-\sigma})c^{*}_{i\sigma}c_{j\sigma}(1-n_{j-\sigma})+H.c.\right]+\frac{4t^2}{U}\sum_{\langle i,j\rangle}\left[\vec{S}_i\cdot\vec{S}_j-\frac{n_i n_j}{4}\right]+H_{3-site} \qquad (1.13)$$

Here H.c. stands for Hermitian conjugate of the first term and $H_{3\text{-}site}$ is the three site term not explicitly written down here. The first term corresponds to the hopping of an electron from an occupied site to an unoccupied site. From (1.13) it can be seen that for $U>>t$ and $n \neq 1$, the system of hopping electrons with onsite interaction only can be interpreted as a system of moving localized moments which are correlated to each other. Whether the system becomes ferromagnetic or anti-ferromagnetic depends on n and U/t.
For some lattice structures, such as for example a carefully chosen closed-packed structure [9], it is even possible to rewrite (1.13) in the form of an effective ferromagnetic Heisenberg model. However just as in the previous case, (1.13) cannot cover the whole story of the $U>>t$ and $n \neq 1$ regime. For some materials in this regime anti-ferromagnetism is predicted by (1.13) while they are actually ferromagnetic. This ferromagnetic tendency can come only from the hopping terms in (1.13). Thus the first logical improvement would be to include next-nearest neighbor hopping or even further ones. In some cases this indeed helps to establish ferromagnetism. However, the question whether orbital degeneracy or extended Hubbard terms are important has to be examined per material.
One should also mention that dilute magnetic alloys and rare earth metals are well described by (1.13) or minor improvements of it.

Thus, for the $U>>t$ limit and for weakly ferro –and anti-ferromagnetic materials, where the band structure is mainly responsible for the magnetic properties, theory may be considered as well established. However, for the intermediate regime, where materials like Ni, Fe and Co are assumed to belong, intensive research is still required. People are trying to develop a so called unified theory [7].
In Chapter 2 it will be explained that the consideration of spin density fluctuations is crucial in understanding the properties of a magnetic system. However, till now only for weak itinerant electron systems these spin density fluctuations can be taken into account appropriately. For stronger interacting systems serious complications occur. It is believed that this problem can be solved by generalizing the picture of spin density fluctuations. This can be understood as follows.
In a local moment system or $U>>t$ regime a spin fluctuation can be seen as the correlated motion of local moments where the local magnitude of the spin fluctuation is constant. For weak itinerant ferromagnets the spin fluctuations are not localized in real space, but in reciprocal space and therefore extent over the whole system. Further, the local magnitude of the spin fluctuation varies with temperature. Another difference is the spatial correlation between spin fluctuations. Due to the large spatial extension of the spin fluctuation in weak itinerant ferromagnets, the spin fluctuations are correlated over a long distance. Further, it can be derived that even above the Curie temperature a short range order persists. This is in contrast with the spin fluctuations in a local moment system which only have small short range correlations below the Curie temperature.
Thus with generalizing the picture of spin density fluctuations is meant that the spin density fluctuations of materials between these limiting cases have a mixture of both

localized and weakly itinerant properties. Neutron scattering experiments already revealed this. For more details see [7].
The properties of the spin density fluctuations can thus also be used to distinguish between different magnetic materials. Whenever they are localized in real space, one speaks of the localized electron magnetism and whenever they are localized in reciprocal space, the situation is referred to as itinerant electron magnetism. For the behavior in between these limiting cases there is no specific name.

Summarizing here, for the strong coupling limit ($U>>t$) well developed theories like the t-J model ($n \neq 1$) and the Heisenberg model ($n=1$) exist, as well as certain modifications of them. In the small and intermediate interaction range, weak itinerant (anti)ferromagnetic materials are well described by Moriya's theory (chapter 2) where the band structure is mainly responsible for magnetism. In between these limiting cases the work is still in progress.

Chapter 2: Itinerant electron magnetism in bulk

In this chapter the most important developments in itinerant electron magnetism in bulk are discussed. First, the derivation of the Hubbard model is explained. With this model as a starting point the Stoner theory will be derived. Then improvements to this theory will be discussed such as the necessity of taking into account the influence of exchange-enhanced spin fluctuations on thermodynamic properties.

2.1 Hubbard model

In this paragraph the Hubbard model is derived which serves as a starting point for the theoretical treatment of itinerant electron magnetism. The system under investigation is a bulk material with periodic lattice structure in which itinerant electrons are responsible for the magnetic properties. Some properties of these itinerant electrons are well described by the tight-binding model [10,11]. From the elementary solid state physics it is known that within this model the states of such electrons should be described by the so called Bloch states. A general expression for a Bloch state is

$$\phi_{\mu k}(\vec{r}) = N_0^{-1/2} \sum_j \sum_m \exp\left(i\vec{k}\cdot\vec{R}_j\right) C_{\mu m} W_m\left(\vec{r}-\vec{R}_j\right), \tag{2.1}$$

where $\phi_{\mu k}(\vec{r})$ is the Bloch state corresponding to the μ'th band, $\vec{k}$ is the wave number, N_0 is the total number of atoms and $\vec{R}_j$ is the position coordinate of the j'th atomic site. From the tight-binding model it is known that the Bloch state can be expressed as a linear combination of a complete set of functions. In this case the Wannier orbitals $W_m\left(\vec{r}-\vec{R}_j\right)$ are chosen which have a local character. A Wannier orbital is the Fourier transform of a Bloch wave.

However, to describe the magnetic properties caused by the itinerant electrons tight-binding theory is not sufficient, because magnetism is a correlation effect. Therefore, an interaction term V is added to the tight binding term H_0. This is a useful approach, because H_0 can then be derived from tight-binding theory. The Hamiltonian of the system will be expressed in second-quantization form. In terms of creation and annihilation operators of Bloch and Wannier states this becomes

$$\begin{aligned} H &= H_0 + V \\ H_0 &= \sum_\sigma \sum_k \sum_\mu \varepsilon_\mu(\vec{k}) a^*_{\mu k\sigma} a_{\mu k\sigma} = \sum_\sigma \sum_{j,l} \sum_{m,m'} t_{jl}^{mm'} c^*_{jm\sigma} c_{lm'\sigma} \\ V &= \frac{1}{2} \sum_{\sigma\sigma'} \sum_{jl} \sum_{j'l'} \sum_{mm'} \sum_{nn'} V_{jl,l'j'}^{mnn'm'} c^*_{jm\sigma} c^*_{\ln\sigma} c_{l'n'\sigma} c_{j'm'\sigma} \end{aligned} \tag{2.2}$$

$$V_{jll'j'}^{mnn'm'} = e^2 \int\int d\vec{r} d\vec{r}' \frac{1}{|\vec{r}-\vec{r}'|} W_m(\vec{r}-\vec{R}_j) W_n(\vec{r}'-\vec{R}_l) W_{n'}(\vec{r}'-\vec{R}_{l'}) W_{m'}(\vec{r}-\vec{R}_j'),$$

where $\varepsilon_\mu(\vec{k})$ is the dispersion of the μ'th band, $t_{jl}^{mm'}$ is the transfer integral between the m'th Wannier orbital at site j and the m''th orbital at site l, $a_{\mu k\sigma}$ is the annihilation operator for the Bloch state and $c_{lm'\sigma}$ is the annihilation operator for the Wannier state.

The H_0 term describes the single particle interactions like the kinetic energy, Coulomb interaction with the ions and some average interaction with all the other electrons in the lattice. For the calculation of these single particle matrix elements, $\varepsilon_\mu(\vec{k})$ and $t_{jl}^{mm'}$, there are several methods which will not be described here [12]. That the Hamiltonian is written in terms of Bloch states is obvious, because this is the general form in which tight-binding theory is presented. The representation in Wannier states becomes useful when examining the interaction term, because then the fact that the Coulomb interaction decreases with increasing distance can be exploited.

The second term V in the Hamiltonian describes the Coulomb interactions between the electrons in the system. It is this term that makes theoretical calculations difficult. Therefore, several approximations are made. One is to take only intra-atomic exchange into account ($j=j'=l=l'$) among which the largest interaction is between the same orbitals ($m=n$ and $m'=n'$):

$$V=\frac{1}{2}\sum_j\sum_\sigma\left\{\sum_{m,m'}U_{mm'}n_{jm\sigma}n_{jm'-\sigma}+\sum_{m\neq m'}\left[(U_{mm'}-J_{mm'})n_{jm\sigma}n_{jm'\sigma}-J_{mm'}c^*_{jm\sigma}c_{jm-\sigma}c^*_{jm'-\sigma}c_{jm'\sigma}\right]\right\}. \tag{2.3}$$

Here $U_{mm'}=V_{jjjj}^{mm'm'm}$ is the Coulomb integral and $J_{mm'}=V_{jjjj}^{mm'mm'}$ the exchange integral. To derive expression (2.3) from (2.2), the Pauli's exclusion principle was also used.

The neglecting of the inter-atomic terms can be justified by the fact that these interactions are screened significantly by the *sp* conduction electrons in transition metals.

A further simplification is to replace $U_{mm'}$ and $J_{mm'}$ by their averages U and J respectively. This leads to

$$V=\frac{1}{2}U\sum_j\sum_{m,m'}\sum_\sigma n_{jm\sigma}n_{jm'-\sigma}+\frac{1}{2}(U-J)\sum_j\sum_{m\neq m'}\sum_\sigma n_{jm\sigma}n_{jm'\sigma}-\frac{1}{2}J\sum_j\sum_{m\neq m'}\sum_\sigma c^*{}_{jm\sigma}c_{jm-\sigma}c^*{}_{jm'-\sigma}c_{jm'\sigma} \tag{2.4}$$

As a final simplification the degeneracy of the band is neglected, which means there is only one quantum number m (or μ). This results in the following expressions for the Hamiltonian in terms of Wannier and Bloch states respectively

$$H=\sum_{j,l}\sum_\sigma t_{jl}c^*_{j\sigma}c_{l\sigma}+U\sum_j n_{j\uparrow}n_{j\downarrow}=\sum_k\sum_\sigma\varepsilon(\vec{k})a^*_{k\sigma}a_{k\sigma}+I\sum_q\sum_k\sum_{k'}a^*_{k+q\uparrow}a^*_{k'-q\downarrow}a_{k'\downarrow}a_{k\uparrow} \tag{2.5}$$

$$I=\frac{U}{N_0}$$

The Hamiltonian in this form is thus called the (single band) Hubbard model and will be used as the starting point in the following paragraphs.

2.2 Stoner theory of itinerant electron magnetism

As mentioned in the previous paragraph, the starting point is the Hubbard model. One of the simplest ways to approximate the interaction term of the Hubbard model even further is to use the Hartree-Fock Approximation (HFA). The HFA is given by

$$n_{j\uparrow}n_{j\downarrow} \xrightarrow{HFA} n_{j\uparrow}\langle n_{j\downarrow}\rangle + n_{j\downarrow}\langle n_{j\uparrow}\rangle - \langle n_{j\uparrow}\rangle\langle n_{j\downarrow}\rangle \tag{2.6}$$

In which the $\langle..\rangle$ denotes the statistical average of the quantity inside the brackets. The statistical average of the occupation number at position *j* with a certain spin direction is replaced by the system average,

$$\langle n_{j\uparrow}\rangle = \langle n_{\uparrow}\rangle = n_{\uparrow} \tag{2.7}$$

Substituting equation (2.6) and (2.7) into the first equation of (2.5) and using the transformation to *k*-space leads to the following Hamiltonian

$$H = \sum_k \sum_\sigma \left(\varepsilon(\vec{k}) + In_{-\sigma}\right) a^*_{k\sigma}a_{k\sigma} + \frac{1}{4}IN^2 - IM^2 \,, \tag{2.8}$$

where *N* is the total number of electrons, *M* is the magnetization in units of $2\mu_B$ and $\sigma = \pm 1$ corresponds to spin up and –down. The last two terms in equation (2.8) come from $U\sum_j \langle n_\uparrow n_\downarrow\rangle = IN_0 \sum_j \langle n_\uparrow n_\downarrow\rangle = I\langle N_\uparrow N_\downarrow\rangle = \frac{1}{4}IN^2 - IM^2$. Here $N_\uparrow$ is the total number of electrons with spin up, and for the last equality $N = N_\uparrow + N_\downarrow$ and $2M = N_\downarrow - N_\uparrow$ is used. These identities for *N* and *M* can also be used to rewrite the single electron energy in the form the Stoner theory is mostly presented:

$$E_{k\sigma} = \varepsilon_k + \sigma\Delta \,,$$
$$\Delta = IM + \frac{1}{2}h \text{ and } h = 2\mu_B\tilde{H} \,. \tag{2.9}$$

From this, 2Δ is the splitting between the spin up and –down band and $\tilde{H}$ is a uniform external magnetic field. Due to this splitting of the bands, there is a difference between the occupation of the spin up and –down band leading to a net magnetization.
Thus within the Stoner theory the system of electrons is approximated as a system of non-interacting particles with single particle energy given by (2.9). This approximation allows the use of the Fermi-Dirac distribution to calculate *N* and *M*;

$$\left.\begin{matrix} N \\ 2M \end{matrix}\right\} = \int dE\rho(E)\left[f(E-\Delta) \pm f(E+\Delta)\right]. \tag{2.10}$$

Here $\rho(E)$ denotes the density of states and $f(x)$ the Fermi-Dirac distribution.

In the following some of the consequences of the Stoner theory are discussed. For this purpose an expression for the free energy is derived first. This can be calculated via the thermodynamic potential of a non-interacting system $(I=0)$:

$$\Omega_0 = -T\sum_{\sigma}\int dE\rho(E)\ln\left(1+\exp\left[-(E+\sigma\Delta-\mu)/T\right]\right)+2\Delta M\ . \tag{2.11}$$

Here T is the temperature in units of energy ($k_B=1$) and μ is the chemical potential. The last term in this equation comes from the constant term in equation (2.8). From this equation an expression for the free energy of a non-interacting system can be obtained by using the following Legendre transformation:

$$F_0(M,T) = \Omega_0 + \mu N\ . \tag{2.12}$$

To obtain the expression of the free energy in the Stoner theory, only a correction term for the exchange energy has to be added. In the case of a uniform external field this is given by

$$F_{HF}(M,T) = F_0(M,T) - IM^2 - hM\ , \tag{2.13}$$

with the last term representing the Zeeman energy. By Taylor expanding $F_0(M,T)$ around $M=0$, the well known Stoner condition for the appearance of ferromagnetism can be derived. This condition is:

$$\alpha_0 \equiv I\rho(E_F) > 1\ . \tag{2.14}$$

Here E_F is the Fermi energy for the paramagnetic state at T=0K.

From (2.13) also an expression for the Curie temperature can be obtained. For this the divergence of the static magnetic susceptibility at the Curie temperature is used, where the static magnetic susceptibility is calculated as

$$\frac{\partial^2 F(M)}{\partial^2 M} = \frac{1}{\chi}, \tag{2.15}$$

where χ is the static magnetic susceptibility in units of $4\mu_B^2$. Therefore the Curie temperature is obtained from the following equation:

$$\left.\frac{d^2 F_{HF}(M,T_c)}{d^2 M}\right|_{M=0} = \frac{1}{\chi_0(T_c)} - 2I = 0. \qquad (2.16)$$

Here χ_0 is the static magnetic susceptibility for a non-interacting system of particles. An expression for this susceptibility can be calculated as follows:

$$\chi_0 \equiv \frac{M}{H} = \int dE \frac{\rho(E)}{2} \cdot \frac{f(E-h/2) - f(E+h/2)}{h}. \qquad (2.17)$$

In case of $h \to 0$ and small temperatures this expression can be approximated by using a Sommerfeld expansion (see paragraph 3.3 below), which leads to

$$\chi_0(T) = \frac{1}{2}\rho(E_F)\left[1 - \frac{\pi^2}{6} R T^2 + ...\right]. \qquad (2.18)$$

Here R is given by: $R = \left(\frac{\rho'}{\rho}\right)^2 - \left(\frac{\rho''}{\rho}\right)\Bigg|_{\mu=E_F}$ with μ the chemical potential and the accent corresponds to the derivative of μ. Finally, the substitution of (2.18) into (2.16) results in the following expression for the Curie temperature:

$$T_c = \left[\frac{6(\alpha_0 - 1)}{\pi^2 \alpha_0 R}\right]^{1/2}. \qquad (2.19)$$

Thus calculated values of T_c for realistic band structures of 3*d* metals are much too high compared with experimental values. For example, a calculation of T_c for Fe, Co and Ni give T_c=4400-6200, 3300-4800 and 2900K respectively, compared with 1040, 1390 and 630K found experimentally [13].

And the last consequence of Stoner theory considered here, is the expression for the static magnetic susceptibility above T_c. This is simply derived from (2.13), (2.15) and (2.18):

$$\frac{1}{\chi} = \frac{\pi^2}{3\alpha_0} IR\left(T^2 - T_c^2\right). \qquad (2.20)$$

This result clearly disagrees with the Curie-Weiss law which is observed in almost all ferromagnets. In Stoner theory the Curie-Weiss behavior is only expected for $T >> E_F$, but not in the realistic temperature range ($T << E_F$).

The success of the Stoner theory is in the explanation of the appearance of ferromagnetism in itinerant electron systems. Further, it also explains the existence of total magnetizations constituted of non-integer number of μ_B per atomic site, arising from the band origin of magnetism (this is not shown in this report) [7,14].

The shortcomings of the theory are the too high predictions of T_c and the wrong temperature dependence of the static magnetic susceptibility.
The failure of the Stoner theory in predicting the Curie temperature and the Curie-Weiss law can be attributed to the HFA of the interaction term. Due to this approximation the itinerant electrons in the system can be seen as moving independently in a common static mean field. In this model the most elementary excitation which disturbs the magnetization of the system is a so called Stoner excitation. A Stoner excitation is a spin flip with possible momentum transfer. To be more precise, this is an excitation of an electron from the majority spin band to the minority spin band with a possible momentum change (figure 2.2.1). Such an excitation costs a large amount of energy, for Fe this is typically of the order eV. Therefore, a lot of thermal energy is required in this model to create enough spin flips to completely destroy the magnetization of the system.

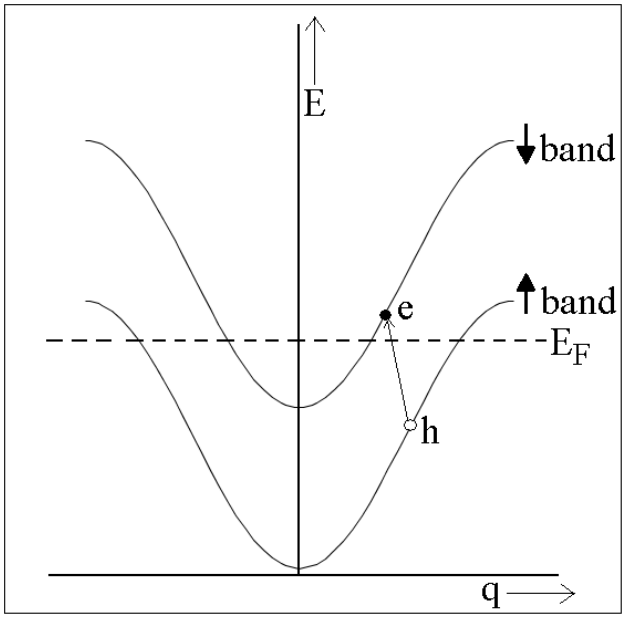

Figure 2.2.1: schematic picture of Stoner excitation where an electron is excited from majority spin up band across the Fermi level to the minority spin down band with possible momentum transfer *q*.

An electron and hole created in the process of a Stoner excitation move independently in a common static mean field. It would be more realistic to include the interactions between the excited electrons and holes. This gives rise to the so-called exchange-enhanced spin density fluctuations including spin waves which can be seen as bound collective modes of electron-hole pairs. In the following paragraphs such improvements to the Stoner theory will be discussed.

2.3 Random phase approximation of spin fluctuations

In the previous paragraph Stoner theory was described where the thermal excitations are the spin flip excitations of electrons across the Fermi surface. These excited electrons and holes move independently in the common static field. This results in rather small spin density fluctuations. For a more realistic approximation, the scattering of electron hole

pairs due to the exchange interaction should be taken into account. In this way exchange enhanced spin density fluctuations such as spin waves will occur.

In this paragraph Stoner excitations are investigated and compared to the exchange enhanced spin density fluctuations. For this purpose one considers the equation of motion of a Stoner excitation:

$$S_+(k,q) = a^*_{k\uparrow} a_{k+q\downarrow} . \tag{2.21}$$

Clearly, this can be seen as an electron with a wave vector $k+q$ and spin down which is excited across the Fermi level into a state with k and spin up. With an additional oscillating external magnetic field, $H_{ext} = \sum_{k'} S_-(k',-q)h_+(q)$, the equation of motion of a Stoner excitation is given by:

$$i\dot{S}_+(k,q) = [S_+(k,q), H + H_{ext}] = (\varepsilon_{k+q} - \varepsilon_k)S_+(k,q) - I\sum_{q'}\sum_{k'}\left(a^*_{k\uparrow}a^*_{k'+q'\uparrow}a_{k+q+q'\downarrow}a_{k'\uparrow} + a^*_{k+q'\uparrow}a^*_{k'-q'\downarrow}a_{k'\downarrow}a_{k+q\downarrow}\right)$$
$$+\left(n_{k\uparrow} - n_{k+q\downarrow}\right)h_+(q) =$$
$$\left[\varepsilon_{k+q} - \varepsilon_k - I\sum_{k'}\left(n_{k'\downarrow} - n_{k'\uparrow}\right)\right]S_+(k,q) + \tag{2.22a}$$
$$I\left(n_{k+q\downarrow} - n_{k\uparrow}\right)\sum_{q'} S_+(k+q',q) - \tag{2.22b}$$
$$I\sum_{q'}\sum_{k'}\left(\left[1-\delta_{kk'}\right]a^*_{k\uparrow}a_{k'\uparrow}a^*_{k'+q'\uparrow}a_{k+q+q'\downarrow} - \left[1-\delta_{k'-q',k+q}\right]a^*_{k'-q'\downarrow}a_{k+q\downarrow}a^*_{k+q'\uparrow}a_{k'\downarrow}\right) + \tag{2.22c}$$
$$\left(n_{k\uparrow} - n_{k+q\downarrow}\right)h_+(q) . \tag{2.22d}$$

In this equation $\hbar = 1$ and for the Hamiltonian equation (2.5), i.e. the Hubbard model, is used. In case the HF-approximated Hubbard model was used, namely the Stoner theory, only (2.22a) and (2.22d) after the second equality-sign would be obtained. This first term gives the kinetic and mean field energy of the Stoner excitation. As a result, the energy spectrum of the Stoner excitation is given by

$$\omega_{Stoner}(k,q) = 2\Delta + \varepsilon_k - \varepsilon_{k+q} , \tag{2.23}$$

where 2Δ is the exchange splitting of the band. In fact, the Stoner excitations only exist in a specific region in ω and q space. To find this region an expression for the transverse dynamic magnetic susceptibility has to be found. Namely, the imaginary part of this susceptibility gives the intensity of the excitation with wave vector transfer q and frequency ω. Within Stoner theory and assuming that $h_+(q)$ oscillates as $e^{i\omega t}$, the following expression for the transverse dynamic magnetic susceptibility $\chi^{+-}_{\Delta 0}(q,\omega)$ can be derived:

$$\frac{\langle S_+(q)\rangle}{h_+(q)} \equiv \chi^{+-}_{\Delta 0}(q,\omega) = \sum_k \frac{\langle n_{k+q\downarrow}\rangle - \langle n_{k\uparrow}\rangle}{\varepsilon_k - \varepsilon_{k+q} + 2\Delta - \omega} = \sum_k \frac{f(\varepsilon_{k+q} - \Delta) - f(\varepsilon_k + \Delta)}{\varepsilon_k - \varepsilon_{k+q} + 2\Delta - \omega}. \quad (2.24)$$

Here $S_+(q)$ is the q'th Fourier coefficient of the spin density $S_x(r)+iS_y(r)$ and $\chi^{+-}_{\Delta 0}(q,\omega)$ is the transverse (denoted by +- in super-script) dynamic magnetic susceptibility within Stoner theory. Further, the sub-script *Δ0* denotes that it is the dynamic magnetic susceptibility within Stoner theory where the electron-electron interaction is only taken approximately into account via the term *IM* (see equation (2.9)). The rest of the electron-electron interaction is neglected which is indicated by the zero, *I=0*, in the subscript. Thus, an expression for the exact dynamic magnetic susceptibility within Hubbard theory is represented by $\chi^{+-}_{\Delta I}(q,\omega)$.

For further computation the summation over k in (2.24) has to be performed, which is done by using the identity

$$\lim_{s\to 0} \frac{1}{x + is} = \frac{P}{x} - i\pi\delta(x), \quad (2.25)$$

with P the Cauchy principal value and $\delta(x)$ the Dirac delta function. To keep things analytical, another approximation has to be made. Therefore equation (2.24) is evaluated for an electron gas model at T=0K, which results in

$$f_{\Delta 0}(q,\omega+is) = \frac{\chi^{+-}_{\Delta 0}(q,\omega+is)}{\chi^{+-}_{00}(0,0)} = \frac{1}{2q}\sum_\sigma^{\pm} \sigma\left[\frac{1}{2}\left(p_\sigma^2 - k_\sigma^2\right)\ln\left|\frac{p_\sigma + k_\sigma}{p_\sigma - k_\sigma}\right| - p_\sigma k_\sigma\right] + i\pi\frac{1}{2}\left(p_\sigma^2 - k_\sigma^2\right)\theta\left(k_\sigma - |p_\sigma|\right), \quad (2.26)$$

$$\begin{aligned} p_\sigma &= \left(2\Delta - \omega - \sigma q^2\right)/2q, \\ k_\sigma &= \left(1 - \sigma\xi\right)^{1/3}, \\ \left.\begin{matrix}\mu \\ \Delta\end{matrix}\right\} &= \frac{1}{2}\left[(1+\xi)^{2/3} \pm (1-\xi)^{2/3}\right], \\ \xi &= 2M/N. \end{aligned} \quad (2.27)$$

In these equations the wave vector is expressed in units of the Fermi vector k_F and the energy in units of the Fermi energy, $E_F = k_F^2/2m$, for the paramagnetic state. Further, the μ is the chemical potential and $\theta(x)$ is the step function.

With the expression of the imaginary part of the susceptibility there, the region where Stoner excitations exist and their intensity can be evaluated. This region and intensity within Stoner theory is shown in figure 2.4.1(a). Here the solid lines represent the intensity contours and the dotted lines give discontinuities coming from the step functions in (2.26). The Stoner excitation at *q=0* represents a pure spin flip without momentum

transfer. Such an excitation is only possible for an energy equal to band splitting between the spin-up and spin-down bands as can be seen in the figure.

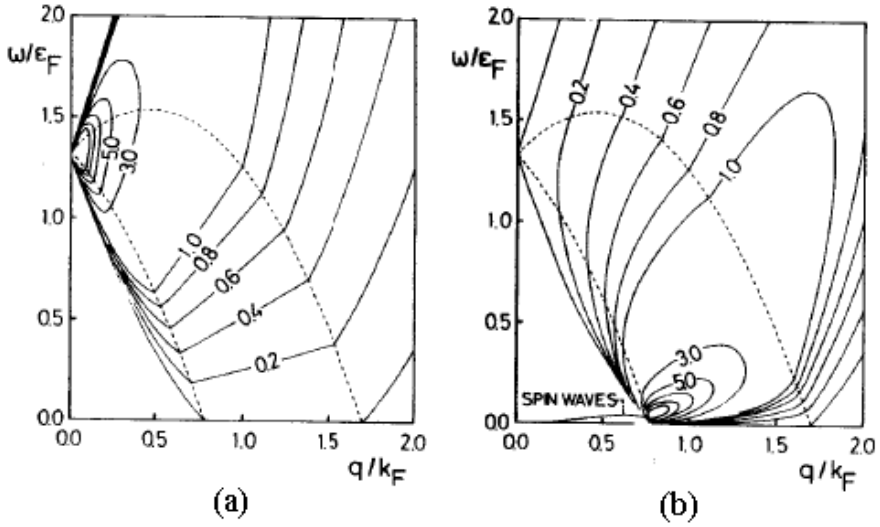

Figure 2.4.1: region in ω and q space where Stoner excitations exist with corresponding intensity contours. (a) For HFA and (b) for HF-RPA. The solid lines represent the intensity contours and the dotted lines discontinuities coming from the step functions [7].

As mentioned before the HFA is a rather poor approximation to describe excitations, because it assumes that a created electron and hole move independently in a common mean field. For a more realistic picture obviously scattering of electron and hole pairs due to the exchange interaction should be taken into account. In equation (2.22) this effect of scattering due to the exchange interaction is given by the second and third terms. The second term takes into account the scattering with conservation of momentum transfer q and the third one the scattering without this conservation. To get a better approximation for the dynamic magnetic susceptibility, the first (2.22a), second (2.22b) and fourth (2.22d) terms are taken into account. What the effect of including the third term (2.22c) is will be discussed in the next paragraph. The expression that is obtained from the Heisenberg equation of motion is

$$\left(\varepsilon_k - \varepsilon_{k+q} + 2\Delta - \omega\right)\left\langle\left\langle S_+(k,q)\right\rangle\right\rangle = \left\langle n_{k+q\downarrow} - n_{k\uparrow}\right\rangle\left[I\left\langle S_+(q)\right\rangle - h_+(q)\right]. \tag{2.28}$$

Here $S_+(q) = \sum_k S_+(k,q)$. From this equation it can be seen that the term in angular brackets after the equality sign is the effect of an oscillating molecular field. This is the reason for calling this approximation the dynamic mean-field approximation or the random-phase approximation (RPA). From equation (2.28) the following expression for the dynamic magnetic susceptibility can be obtained

$$\chi^{+-}_{RPA}(q,\omega) = \frac{\chi^{+-}_{\Delta 0}(q,\omega)}{1 - I\chi^{+-}_{\Delta 0}(q,\omega)}. \tag{2.29}$$

Here $\chi^{+-}_{\Delta 0}(q,\omega)$ is the dynamic magnetic susceptibility within the HFA calculated before (see (2.24)). Thus from (2.29) it can be seen that $\chi^{+-}_{RPA}(q,\omega)$ has an imaginary part in the same region as $\chi^{+-}_{\Delta 0}(q,\omega)$, however the intensity differs due to the denominator. Remember that this denominator originates from the effect of the exchange enhancement of spin fluctuations. Another consequence of this denominator is the existence of poles on the real frequency axis, where no Stoner excitations exist. This means that these poles do not correspond to single excitations, but to collective excitations called spin waves. The intensity contours and dispersion of the spin waves within HF-RPA are given in figure 2.4.1(b). The dispersion of the spin waves can be found from

$$1 - I\,\mathrm{Re}\left(\chi^{+-}_{\Delta 0}(q,\omega_q)\right) = \chi^{+-}_{\Delta 0}(0,0) - \mathrm{Re}\left(\chi^{+-}_{\Delta 0}(q,\omega_q)\right) = 0\,. \tag{2.30}$$

The second equality is found by using the fact that in the absence of anisotropy the static transverse susceptibility diverges in ferromagnets. From (2.30) the following dispersion for spin waves for small q and ξ (see (2.27)) can be found

$$\begin{aligned} \omega_q &= Dq^2\left(1-\eta q^2+\ldots\right), \\ D &= \frac{1}{9}\xi\left(1+\frac{32}{135}\xi^2+\ldots\right) \\ \eta &= \frac{3}{4\xi^2}+\ldots \end{aligned} \tag{2.31}$$

In figure 2.4.1 (b) the spin wave dispersion and the intensity contours of the Stoner excitations for the electron gas model are shown. The intensity of the spin waves is calculated from the residue of the pole. This intensity is the largest at $q=0$ and decreases towards zero when the Stoner boundary is approached.

Critical spin fluctuations

In this subparagraph spin fluctuations near the Curie temperature and for weak ferromagnets are discussed. A weak ferromagnet is a material with a Curie temperature close to zero (see paragraph 1.2.3 above). It is good to discuss weak ferromagnets here within HF-RPA, because in the next paragraph an improved HF-RPA will be discussed which is only valid for such weak ferromagnets.

Near the Curie temperature and for weak ferromagnets the essential spin fluctuations are those with a long wavelength (small q) and small frequency ω. In the following this will be quantified. For this purpose the dynamic magnetic susceptibility $\chi^{-+}_{\Delta 0}(q,\omega)$ is expanded in small ω and q (and Δ), where small means $\omega << E_F$ and $q << k_F$. The expansion looks as follows

$$
\begin{aligned}
& f_{\Delta 0}(q,\omega) = \chi^{-+}_{\Delta 0}(q,\omega) / \chi^{-+}_{00}(0,0) = 1 - Aq^2 - B(\omega/q)^2 + ... \\
& + \Delta\left[D_1(\omega/q^2) + D_2\omega + D_3(\omega^3/q^4) + ...\right] \\
& - \frac{1}{2}\Delta^2\left[F_1 + F_2(\omega/q^2)^2 + F_3 q^2 + F_4(\omega/q)^2 + F_5(\omega^4/q^6) + ...\right] \\
& + ... + iC\omega/q + ...
\end{aligned}
\tag{2.32}
$$

The coefficients in this expansion can be calculated from the band structure near the Fermi surface. For the electron gas model these coefficients are well known and are

$$
\begin{gathered}
A=1/12,\quad B=1/4,\quad C=\pi/4,\quad D_1=1/2,\quad D_2=1/24,\quad D_3=1/8, \\
F_1=1/3,\quad F_2=1/2,\quad F_3=1/30,\quad F_4=F_5=1/4.
\end{gathered}
\tag{2.33}
$$

In the paramagnetic phase ($T>T_c$) without external field the dynamic magnetic susceptibility in HF-RPA is given by

$$
f_{RPA}(q,\omega) = \frac{f_{00}(q,\omega)}{1 - \alpha \cdot f_{00}(q,\omega)}. \tag{2.34}
$$

Here $\alpha = I\chi^{-+}_{00}(0,0)$. Now substituting (2.32) into (2.34) results in

$$
f_{RPA}(q,\omega) = \frac{1}{\alpha}\frac{1 - Aq^2 - B(\omega/q)^2 + iC\omega/q}{\left[(1-\alpha)/\alpha\right] + Aq^2 + B(\omega/q)^2 - iC\omega/q}. \tag{2.35}
$$

From this equation can be seen that when α is close to 1 the dynamic magnetic susceptibility is enhanced strongly for small ω and q. For weak ferromagnets and temperatures close to T_c, α is close to 1. This can be seen from the static magnetic susceptibility within HF-RPA which is obtained from equation (2.22) by setting $\omega=q=0$. At the Curie temperature the static magnetic susceptibility diverges or $1 - I\chi_0(T_c) = 0$. Thus, from this and (2.18) follows that α is approximately equal to 1.

Summarizing here, the Stoner theory predicts the ground state quite well, but gives a poor description of excitations. This is because only Stoner excitations are taken into account. As an improvement, the exchange enhancement of spin fluctuations was taken into account by calculating them around the HFA equilibrium state, which resulted in a good description of excitations around the ground state. However their influence on the thermal equilibrium state is not taken into account yet in the HF-RPA. Therefore this theory has the same shortcomings in predicting thermodynamic properties at finite temperatures as the Stoner theory. Thus a logical improvement of the HF-RPA would be to take the influence of the exchange enhanced spin fluctuations on the thermal equilibrium state into account. This would give better predictions for low temperatures only, because the spin fluctuations in HF-RPA were calculated around T=0K and the Stoner equilibrium state. How to improve this theory even further to give better predictions also at the elevated temperatures will be discussed in the next paragraph.

2.4 Self-Consistent Renormalization (SCR) Theory of Spin Fluctuations

In this paragraph an improvement to the HF-RPA is discussed. This improvement is to take into account the influence of the exchange-enhanced spin density fluctuations on the free energy of the thermal equilibrium state. Therefore one should start with an exact expression of the free energy of an interacting system of particles, which can be written as

$$F = F_0 + \Delta_I F\,. \tag{2.36}$$

Here $\Delta_I F$ is the correction term to the free energy of a system of non-interacting particles. In the following it will be shown that this correction term can be expressed in terms of the transverse dynamic magnetic susceptibility of the whole system. For this purpose one can use the following expression for the free energy as a function of *I*:

$$\exp\left[-F(I)/T\right] = Tr\left(\exp\left\{-\left[H_0 + V(I)\right]/T\right\}\right). \tag{2.37}$$

Here *Tr(…)* stands for the trace and *V(I)* is the interaction term of the Hubbard Hamiltonian. Of this expression the derivative with respect to *I* can be taken, which leads to

$$\frac{\partial F(I)}{\partial I} = Tr\left\{\left(\frac{\partial V}{\partial I}\right)\exp\left(\left[F(I) - H_0 - V(I)\right]/T\right)\right\} = \left\langle\frac{\partial V}{\partial I}\right\rangle_I . \tag{2.38}$$

Integrating this expression from *0* to *I* gives

$$F(I) = F_0 + \int_0^I dI' \left\langle\frac{\partial V}{\partial I}\right\rangle_{I'} \Rightarrow \Delta_I F = \int_0^I dI' \left\langle\frac{\partial V}{\partial I}\right\rangle_{I'}, \tag{2.39}$$

with $\langle ... \rangle_I$ the statistical average at fixed *I*. The following step is to rewrite the Hubbard Hamiltonian as

$$\begin{aligned} H &= H_0 + V(I), \\ H_0 &= \sum_k \sum_\sigma \varepsilon_k a^*_{k\sigma} a_{k\sigma}, \\ V(I) &= \frac{1}{2} NU - \frac{1}{2} I \sum_q \left[S_-(q), S_+(-q)\right]_+ . \end{aligned} \tag{2.40}$$

Here $[\ldots]_+$ is the anti-commutator operator, $S_-(q) = \sum_k a^*_{k\downarrow} a_{k+q\uparrow}$ and $S_+(-q) = \sum_k a^*_{k\uparrow} a_{k-q\downarrow}$. Substituting (2.40) into (2.39) gives

$$\Delta_I F = \frac{1}{2} NU - \frac{1}{2} \int_0^I dI \sum_q \left\langle \left[S_-(q), S_+(-q) \right]_+ \right\rangle_I . \tag{2.41}$$

In general it is more convenient for magnetism problems to calculate *F(M,T)*, which is the free energy of the total system as a function of *M*, *I* and *T*. This is given by

$$\begin{aligned} &F(M,T) = F_0(M,T) + \Delta_I F(M,T), \\ &\Delta_I F(M,T) = \int_0^I dI \left\langle \frac{\partial V}{\partial I} \right\rangle_{M,I} = \frac{1}{2} NU - \frac{1}{2} \int_0^I dI \sum_q \left\langle \left[S_-(q), S_+(-q) \right]_+ \right\rangle_{M,I} . \end{aligned} \tag{2.42}$$

Here $\langle ... \rangle_{M,I}$ indicates the statistical average under fixed values of *M* and *I*. By using fluctuation-dissipation theory, the spin correlation function of (2.42) can be written in terms of the transverse dynamic magnetic susceptibility as

$$\begin{aligned} &\left\langle \left[S_-(q), S_+(-q) \right]_+ \right\rangle = \frac{1}{\pi} \int_{-\infty}^{\infty} d\omega \cdot \cosh(\omega / 2T) \, \mathrm{Im}[\chi^{-+}_{MI}(q, \omega + is)], \\ &\chi^{-+}_{MI}(q, \omega + is) = i \int_0^{\infty} dt \cdot e^{i\omega t} \left\langle \left[S_-(q,t), S_+(-q,0) \right] \right\rangle_{M,I} . \end{aligned} \tag{2.43}$$

Here $\chi^{-+}_{MI}(q, \omega + is)$ is the exact transverse dynamic magnetic susceptibility of the system. Inserting (2.43) into equation (2.42) and neglecting the constant term one obtains the following exact correction term to the free energy of a system of non-interacting particles:

$$\Delta_I F(M,T) = -\frac{1}{2\pi} \int_{-\infty}^{\infty} d\omega \coth(\omega / 2T) \sum_q \int_0^I dI \, \mathrm{Im}[\chi^{-+}_{MI}(q, \omega + is)] . \tag{2.44}$$

From this equation it is possible to calculate the correction term within HFA, which was calculated in paragraph 2.3 equation (2.13). This is done by taking *I=0* in (2.44) (or (2.39)). The result is that $\left\langle \partial V / \partial I \right\rangle_{M,0} = N_0 \sum_j \left\langle n_\uparrow n_\downarrow \right\rangle_{M,0} = \left\langle N_\uparrow N_\downarrow \right\rangle_{M,0} = \frac{1}{4} N^2 - M^2$. Integrating over *I* gives the HFA correction term. Therefore another convenient form of writing the total free energy could be as follows

$$F(M,T) = F_{HF}(M,T) + \Delta F(M,T),$$
$$\Delta F(M,T) = -\frac{1}{2\pi}\int_{-\infty}^{\infty} d\omega \cdot \coth(\omega/2T) \sum_q \int_0^I dI \left[\chi_{MI}^{-+}(q,\omega+is) - \chi_{M0}^{-+}(q,\omega+is)\right] \tag{2.45}$$

From the correction terms in equations (2.44) and (2.45) it can be clearly seen how the influence of exchange-enhanced spin density fluctuations on the free energy can be taken into account.

As a first improvement of the HF-RPA, the expression for $\chi_{MI}^{-+}(q,\omega+is)$ in (2.45) could be approximated by $\chi_{RPA}^{-+}(q,\omega+is)$. This improvement would be plausible only for low temperatures, because the excitations were calculated for T=0K and the HFA ground state. It is clear however, that the HFA ground state is changed by the influence of the spin density fluctuations. In its turn the changed ground state influences the spin density fluctuations. However by just taking $\chi_{RPA}^{-+}(q,\omega+is)$ for $\chi_{MI}^{-+}(q,\omega+is)$ the effect of this changed ground state on the spin density fluctuations is not taken into account.

In order to assure that the influence of the changed ground state on the spin density fluctuations is taken into account and predictions can be done at elevated temperatures, the theory should be made self consistent. With self consistent is meant that the long wavelength and small frequency limit of the dynamic magnetic susceptibility $\chi_{MI}^{-+}(q,\omega)$ does agree with the static magnetic susceptibility calculated from the renormalized free energy via (2.15). Therefore, a formally exact expression for the transverse dynamic magnetic susceptibility can be written first:

$$\chi_{MI}^{-+}(q,\omega) = \frac{\overline{\chi}_{MI}^{-+}}{1 - I\overline{\chi}_{MI}^{-+}} = \frac{\chi_{M0}^{-+}(q,\omega)}{1 - I\chi_{M0}^{-+}(q,\omega) + \lambda_{MI}(q,\omega)}. \tag{2.46}$$

Here $\overline{\chi}_{MI}^{-+} = \overline{\chi}_{MI}^{-+}(q,\omega) = \dfrac{\chi_{M0}^{-+}(q,\omega)}{1+\lambda_{MI}(q,\omega)}$. In this equation λ takes into account the exact corrections to the RPA or the neglected term of equation (2.22). This λ can be found by exploiting the condition that the theory should be self consistent. To simplify the calculation, λ is approximated by its static long wavelength limit. This approximation is assumed to be valid for the weakly ferromagnetic case, because then $\lambda << I\chi_{M0}^{-+}(0,0) \approx 1$. There is no rigorous proof for this approximation, but it can be made plausible. For this purpose first the static long wave-length of (2.46) is taken. At the Curie temperature the static magnetic susceptibility diverges or with other words $1 - I\chi_{00}^{-+}(T_c) + \lambda_{0I}(T_c) = 0$. From this and the fact that the weakly ferromagnetic case is considered (Curie temperature close to zero) it follows that $\lambda_{0I}(0) = I\chi_{00}^{-+}(0) - 1 \approx 0$. Now assuming that for $\lambda_{MI}(q,\omega)$ a similar expansion as in (2.32) is possible, the long wave-length and low frequency contributions of $\lambda_{MI}(q,\omega)$ will be enhanced strongly. Therefore, the approximation $\lambda_{MI}(q,\omega) \approx \lambda_{MI}(0,0)$ is made.

The term $\lambda_{MI}(0,0)$ can be found self consistently from the following two equations which hold under an external magnetic field:

$$\frac{\partial^2 F(M,I)}{\partial^2 M} = \frac{\partial^2 F_0(M,T)}{\partial^2 M} - 2I + \frac{\partial^2 \Delta F(M,T)}{\partial^2 M}, \tag{2.47}$$

$$\frac{1}{\chi_{MI}^{-+}(0,0)} = \frac{\left[1+\lambda_{MI}(0,0)\right]}{\chi_{M0}^{-+}(0,0)} - I\,. \tag{2.48}$$

These two equations lead to

$$\lambda_{MI}(0,0) = \chi_{M0}^{-+}(0,0)\left(\frac{\partial^2 \Delta F(M,T)}{\partial^2 M}\right). \tag{2.49}$$

In this equation the term between the brackets depends on $\lambda_{MI}(0,0)$ as well. Therefore, the next step would be to evaluate this term. For this purpose more approximation are needed, which can not be mathematically justified on forehand, but should be checked afterwards [7]. These approximations will be that:
(1) $\partial\lambda_{MI}/\partial I$ is neglected compared with $\chi_{M0}^{-+}(0,0)$ in computing the integral over I in the expression of ΔF,
(2) $\partial\lambda_{MI}/\partial M$ will be neglected compared with $I\cdot\partial\chi_{M0}^{-+}(0,0)/\partial M$ in evaluating the first derivative to M and
(3) $\partial^2\lambda_{MI}/\partial^2 M$ will be neglected compared to $I\cdot\partial^2\chi_{M0}^{-+}(0,0)/\partial^2 M$ in the calculation of the second derivative to M.
Basically this means that it is assumed that $\lambda_{MI}(\omega,q)$ is in good approximation independent of ω, q, M and I, which is assumed to be the case in the weakly ferromagnetic limit. Using these approximations to evaluate equation (2.49) gives in the paramagnetic phase ($T>T_c$)

$$\begin{aligned}
&\lambda(T,\delta) = \frac{1}{2\pi}\int_{-\infty}^{\infty} d\omega\cdot\coth(\omega/2T)\,\mathrm{Im}\{G(\omega+is,\delta)\},\\
&G(\omega,\delta) = -\alpha\chi_0\sum_q\left[\frac{f_M(\partial^2 f_M/\partial^2 M)}{\delta+1-f_M} + \frac{(1+\delta)(\partial f_M/\partial M)^2}{(\delta+1-f_M)^2}\right]_{M=0}.
\end{aligned} \tag{2.50}$$

Here $\alpha = I\chi_{00}^{-+}(0,0)$, χ_0 is the static magnetic susceptibility for a non-interacting system of electrons, $f_M = \chi_{M0}^{-+}(q,\omega)/\chi_{00}^{-+}(0,0)$ and δ is given by

$$\frac{\chi_0}{\chi} \equiv \alpha\delta = 1-\alpha+\lambda(T,\delta)\,, \tag{2.51}$$

with χ the static magnetic susceptibility above the Curie temperature. This equation is obtained from (2.46) and is valid for temperatures above the Curie temperature.

In the following an expression for the Curie temperature will be derived. The Curie temperature follows from

$$1-\alpha(T_c)+\lambda(T_c,0)=0, \tag{2.52}$$

which is obtained from the divergence of the static magnetic susceptibility at the Curie temperature. A similar expression was used to explain that $\lambda << I\chi_{00}^{-+}(0,0)\approx 1$, but here λ still depended on *I*.
To obtain an expression for T_c, first equation (2.50) has to be evaluated. This evaluation is greatly simplified by noticing that the most important effect of the exchange enhancement arises from the region of small q and ω at T_c, where $\delta=0$. Therefore the expansion of f_M in terms of q and ω of equation (2.32) (and the expansion coefficients of (2.33)) will be used.

From (2.32) an expression for f_M, $\partial f_M/\partial M$ and $\partial^2 f_M/\partial^2 M$ in the paramagnetic phase can be found in principle. However, it is convenient to change first the variables from *M* to *B=h(M)*. Then expression (2.50) becomes

$$\begin{aligned}
\lambda(T,\delta) &= \frac{1}{2\pi}\int_{-\infty}^{\infty} d\omega\cdot\coth(\omega/2T)\,\mathrm{Im}\{G(\omega+is,\delta)\},\\
G(\omega,\delta) &= -\frac{\alpha}{\chi_0}\sum_q\left[\frac{f_M\left(\frac{\partial^2 f_M}{\partial^2 B}\right)}{\delta+1-f_M}+\frac{(1+\delta)\left(\frac{\partial f_M}{\partial B}\right)^2}{(\delta+1-f_M)^2}\right]_{B=0}
\end{aligned} \tag{2.53}$$

The expressions for f_M, $\partial f_M/\partial B$ and $\partial^2 f_M/\partial^2 B$ in the paramagnetic phase can now be calculated from (2.32) and become approximately

$$\begin{aligned}
&f_0(\omega,q)=1-Aq^2+iC\omega/q\\
&\left[\partial f_0(\omega,q)/\partial B\right]_{B=0}=D_1(\omega/q^2)+D_2\omega+D_3(\omega^3/q^4)\\
&\left[\partial^2 f_0(\omega,q)/\partial^2 B\right]_{B=0}=-F_1-F_2(\omega^2/q^4)-F_3q^2
\end{aligned} \tag{2.54}$$

The following step is to substitute the expressions of (2.54) into (2.53) and calculate *G(ω,0)*. For this calculation the sum over q is replaced by an integral. It is important to restrict $|q|$ within a proper cut off value q_c to keep the model consistent with the single band assumption. For small ω, Im(*G(ω,0)*) becomes,

$$\mathrm{Im}(G(\omega+is,0)=w_0\left[\Gamma_1\omega^{1/3}-\Gamma_2\omega\ln\omega+O(\omega)\right],$$

$$
\begin{aligned}
&w_0 = V / 4\pi^2 \rho(E_F),\\
&\Gamma_1 = \left(\pi / 3\sqrt{3}\right)(C / A)^{1/3}\left[\alpha F_1 / A - \frac{2}{3}\left(D_1 / C\right)^2\right],\\
&\Gamma_2 = \frac{1}{3}\left\{\alpha\left(2F_2 / C + F_3 C / A^2\right) - 4BD_1^2 / C^3\right\}.
\end{aligned}
\tag{2.55}
$$

Here V is the volume of the crystal. The next step is to calculate $\lambda(T,0)$. For this purpose equation (2.53) is rewritten as

$$
\begin{aligned}
&\lambda(T,0) = \lambda_0 + \lambda_1,\\
&\lambda_0 = \frac{1}{2\pi}\int_{-\infty}^{\infty} d\omega \cdot sign\{\omega\} \cdot \mathrm{Im}\left(G(\omega + is,0)\right),\\
&\lambda_1 = \frac{1}{2\pi}\int_{-\infty}^{\infty} d\omega \cdot sign\{\omega\} \cdot \frac{2}{e^{\frac{|\omega|}{T}} - 1} \cdot \mathrm{Im}\left(G(\omega + is,0)\right),
\end{aligned}
\tag{2.56}
$$

where sign{…} is the signum function. The first term, λ_0, in this equation depends relatively weakly on temperature via α. Therefore this term can be seen as the contribution of the zero point fluctuations, because it remains finite at T=0K. However the second term, λ_1, is strongly temperature dependent via the Bose factor and vanishes for $T \to 0$K. In λ_0 the high frequency contributions are dominant. In contrast, the low frequency contributions are obviously dominant in λ_1.

In fact, an expression for $G(\omega,0)$ valid over the whole ω range should be used to calculate λ_0, which makes numerical work elaborate. In the following λ_0 will be assumed to be constant and is included into α of equation (2.52). This assumption is plausible, because its temperature dependence is very weak compared with λ_1.

For low temperatures it is sufficient to use the approximation $\mathrm{Im}(G(\omega + is,0) = w_0 \Gamma_1 \omega^{1/3}$ to calculate λ_1. This leads to the following expression for λ_1:

$$
\lambda_1 = \frac{2}{\pi} w_0 \int_0^{\infty} d\omega \left(e^{\omega / T} - 1\right)^{-1} \Gamma_1 \omega^{1/3} = w_0 \left(2\Gamma_1 / \pi\right) T^{4/3} \xi(4/3)\Gamma(4/3)\,. \tag{2.57}
$$

Here $\xi(x)$ and $\Gamma(x)$ are the well known zeta and gamma functions respectively [15]. From this equation it can be seen that λ_1 indeed has much stronger temperature dependence than that of α. Therefore, in good approximation the temperature dependence of α in equation (2.52) can be neglected compared to that of λ_1. This results in the following expression for the Curie temperature

$$
T_c = \left[\pi(\alpha_0 - 1) / 2 w_0 \Gamma_1 \xi(4/3)\Gamma(4/3)\right]^{3/4} \tag{2.58}
$$

This Curie temperature is generally lower than that calculated within Stoner theory. Further, experimentally this equation is also supported. Experiments on $Ni_{1-x}Pt_x$ show $T_c^{\exp} \sim (\alpha - 1)^{0.7}$ and on $(Ni_{1-x}Pd_x)_3Al$ show $T_c^{\exp} \sim (\alpha - 1)^{0.75}$ [16,17].

Another success of this SCR-theory is that it predicts that the magnetic susceptibility obeys an approximate Curie-Weiss law, for a derivation of this, see [7,18]. Further this theory also predicts corrections to the magnetization below the Curie temperature as compared with the Stoner theory [1,19].

Chapter 3: Curie temperature of small itinerant-electron clusters

3.1 SCR-theory for cluster systems

In the previous chapter it was explained step by step how to treat a weak itinerant electron bulk system. A proper description of the spin density fluctuations and their influence on the thermodynamic equilibrium state appeared to be crucial. The best way to obtain this is by calculating them self consistently. The result of this treatment or SCR-theory was a much better prediction of the Curie temperature as well as other magnetic properties compared to the Stoner theory. In this chapter the SCR-theory is used to obtain an expression for the Curie temperature of a cluster system. These results will be compared with the bulk limit treated in the previous chapter. In this paragraph it is explained what the general difference is between SCR-theory for bulk and for cluster systems.
The cluster system under investigation was described in the introduction and will be shortly recapped here. A cluster is an almost spherical particle having microscopic (atomic) variations at the surface. A cluster system is then a collection of clusters of the same size, but differing in the surface irregularities. It is further assumed that the electrons responsible for the magnetic properties are itinerant ones, and that spin-orbit coupling can be neglected. Another important assumption was made about the sizes of the clusters under investigation. Only clusters containing approximately 100 atoms or more are considered. The derivation of this limitation will be explained in paragraph 3.5.

From paragraph 2.4 it is clear that in principle only the dynamic magnetic susceptibility of a non-interacting system has to be calculated in order to use the SCR-theory for the approach of the Curie temperature from above. Namely, from this quantity the static magnetic susceptibility can be calculated by taking $\omega=q=0$ limit and λ can be calculated by using the self consistency condition.
A cluster differs from a bulk system by its size and the presence of a surface. Due to these two differences the energy spectrum of a cluster system completely differs from that of a bulk system. The dynamic magnetic susceptibility is depended on the energy spectrum and will therefore differ from bulk. Actually, it will become clear in paragraph 3.4 that for our purposes it only depends on the energy levels around the Fermi level.
Thus the first problem that must be handled is the way the energy spectrum of a cluster system is approached. This will be explained in the next paragraph. When this is known, an expression for the dynamic susceptibility could be calculated and from this the static magnetic susceptibility and λ. However, the calculation of the dynamic magnetic susceptibility is quite difficult and will be done only for certain limits. This is done in paragraph 3.4. In paragraph 3.3 the static susceptibility will be calculated via the free energy. Finally, in paragraph 3.5 there will be derived what happens with the Curie temperature of an itinerant cluster system

3.2 Random Matrix Theory

In this paragraph it is described how the electronic structure of a cluster system can be interpreted. For this purpose mainly the work of Kubo and improvements of it will be followed [1,2,20].

For macroscopic-size objects at high temperatures the single-electron energy spectrum can be considered to be continuous. However, for systems of finite size like clusters there will be a temperature range, $k_bT<<\delta$, where the discreteness of the single-electron states appears. Here δ is the average energy level spacing around the Fermi level. The symbol δ was also used in equation (2.47), but distinction between these two will be clear from the context. In the regime of $k_bT<<\delta$ the discreteness will affect the static thermodynamic properties. To calculate these thermodynamic properties of a cluster system, the distribution of energy levels near the Fermi energy is required. Such a distribution will be finally derived in this paragraph and will be then used to calculate the static magnetic susceptibility in the next paragraph. First, however, the ideas behind the discrete treatment of the energy levels and its validness are discussed.
For the clusters under investigation is assumed that they are large enough so that around the Fermi level the average energy level spacing increases inversely with the cluster's volume. This is known from the work of H. Weyl [21,22], where it is shown that for large quantum numbers the density of eigen-values depends on the volume of the region only. This also means that this density does not depend on the exact imposed boundary conditions. Considering the free electron gas model, where the Fermi energy is only dependent on the electron density n, this results in

$$\delta \propto \frac{1}{V} \propto \frac{E_F}{N}. \tag{3.1}$$

Here N is the total number of electrons. Another important aspect is the broadening of the energy levels due to the finite life time. Kubo used the Fermi liquid theory to describe the electrons in a cluster. This theory takes electron-electron and electron-phonon interactions approximately into account. In this way the electron system can be approximated by a collection of non-interacting quasi-particles of which the level broadening can be neglected at low temperatures. This means that for reasonable cluster sizes the restriction $k_bT<<\delta$ is stronger than the restriction that the level broadening has to be small compared to the average level spacing.
Kubo also discussed the neutrality of a cluster system. For this he compared the work function of a cluster with the thermal fluctuations. The work function in classical electrodynamics can be approximated by

$$W \approx \frac{e^2}{R} = \frac{1.5 \cdot 10^5 k_b}{R} \text{KÅ}. \tag{3.2}$$

Here W is the work function and e is the elementary unit of charge. Thus, for $k_bT<<\delta$ the cluster system can be treated as neutral. This justifies the later use of the canonical ensemble. However, for exact treatment the grand canonical ensemble must be used and

this interaction must be included. In the paper of Denton, Mühlschlegel and Scalapino (reference [20]) it is shown that at any case this gives only minor corrections at low temperatures.
And the last point to mention before going into details of the energy spectrum treatment of a cluster system, is that there is a difference between an even and odd number of electrons in a cluster at low temperatures. This has to do with the exact counting of excitations. Namely, at low temperatures only a few energy levels around the Fermi level have to be taken into account and therefore even and odd particles have a different number of excitations.

Thus, a cluster is treated as an almost spherical particle with atomic surface irregularities. For a system of non-interacting quasi-particles enclosed in a perfect sphere the energy spectrum can be easily calculated. Highly degenerate energy levels will be encountered due to the high symmetry. This symmetry comes from the geometry of the system. However in reality there is this atomic surface roughness which will cause the degenerate energy levels to split apart. With other words the energy spectrum of the quasi-particles in a single cluster is determined by its exact geometry. Other clusters with the same volume, but with different shape will have different energy spectra, but the same average distance between energy levels at the Fermi level. For a cluster knowing the exact geometry comes down to knowing it with atomic precision. Therefore, the complex geometry has to be treated in some approximate form. How this is done will be explained below.

The atomic surface roughness of the cluster can be interpreted as a random potential which causes the splitting of the degenerate energy levels expected from a perfect spherical cluster. To account for this randomness a collection of clusters of the same size, but with different surface irregularities is considered. Random matrix theory says that the Hamiltonian of each cluster in this collection can be approximated by a randomized matrix. The energy distribution for the entire collection of clusters is then obtained by diagonalizing the collection of matrices.
It is thus plausible to approximate a cluster with a random matrix. Namely, the part of the Hamiltonian corresponding to the energy levels around the Fermi level can be approximated by a random matrix. For this it is important to go into more detail of the splitting of the energy levels by a random potential referring to the atomic surface irregularities. From the text above it seems that all the energy levels are split apart by the random potential. However, in the field of quantum chaos it is well known that only the high energy states are split apart [23]. One can understand this qualitatively. The low lying states correspond to quasi-particles with large wavelengths which cannot 'see' or are not sensitive to the irregularities of atomic size at the surface. For the higher energy states which correspond to quasi-particles with wavelengths of the order of $1/d_{atom}$ (d_{atom} is the diameter of an atom), one could expect that the atomic surface roughness becomes 'visible' and will disturb the states. For the following the assumption is made that states at the Fermi level only mix with each other due to the surface roughness. Thus, to put everything in a more quantitative form one can write the Hamiltonian of a cluster as

$$H = H_0 + V_{surface} . \tag{3.3}$$

Here H_0 is the Hamiltonian of the perfect spherical cluster, which can be solved in principle or can be diagonalized, and $V_{surface}$ is the matrix corresponding to the surface roughness. The result of this is as follows

$$H_0 = \begin{vmatrix} E_1 & 0 & 0 & 0 & 0 & 0 & 0 & 0 & 0 & 0 & 0 \\ 0 & .. & 0 & 0 & 0 & 0 & 0 & 0 & 0 & 0 & 0 \\ 0 & 0 & E_1 & 0 & 0 & 0 & 0 & 0 & 0 & 0 & 0 \\ 0 & 0 & 0 & .. & 0 & 0 & 0 & 0 & 0 & 0 & 0 \\ 0 & 0 & 0 & 0 & E_F & 0 & 0 & 0 & 0 & 0 & 0 \\ 0 & 0 & 0 & 0 & 0 & .. & 0 & 0 & 0 & 0 & 0 \\ 0 & 0 & 0 & 0 & 0 & 0 & E_F & 0 & 0 & 0 & 0 \\ 0 & 0 & 0 & 0 & 0 & 0 & 0 & .. & 0 & 0 & 0 \\ 0 & 0 & 0 & 0 & 0 & 0 & 0 & 0 & E_n & 0 & 0 \\ 0 & 0 & 0 & 0 & 0 & 0 & 0 & 0 & 0 & .. & 0 \\ 0 & 0 & 0 & 0 & 0 & 0 & 0 & 0 & 0 & 0 & E_n \end{vmatrix}. \tag{3.4}$$

In this matrix E_1 is the lowest lying state and E_n the highest lying state. With the assumption that the states at the Fermi level only mix with each other, then the problem to solve becomes:

$$H = \begin{vmatrix} E_F & .. & 0 \\ .. & .. & .. \\ 0 & .. & E_F \end{vmatrix} + \begin{vmatrix} V_{11} & .. & V_{1N} \\ .. & .. & .. \\ V_{N1} & .. & V_{NN} \end{vmatrix} \rightarrow H = \begin{vmatrix} H_{11} & .. & H_{1N} \\ .. & .. & .. \\ H_{N1} & .. & H_{NN} \end{vmatrix}. \tag{3.5}$$

Here N is the degeneracy of the Fermi level. For the last expression E_F is set equal to zero, because it acts only as a reference state. As mentioned above, the matrix corresponding to the surface irregularities can be interpreted as a random potential or random matrix according to random matrix theory. This random matrix is however restricted in the sense that it must have certain basic symmetry properties which each individual Hamiltonian of a cluster has. These symmetry properties depend on the relative magnitude of the spin-orbit coupling H_{so} and the external magnetic field $\mu_B \tilde{H}$ compared to the average level spacing δ. For small H_{so} and $\mu_B \tilde{H}$ compared to δ for example, the system has time-reversal and rotational invariance. The other possibilities are given in table 3.2.1.

These two conditions obtained from the relative magnitude of H_{so} and $\mu_B \tilde{H}$ compared with δ, impose certain properties to the matrices. Further, the matrix elements corresponding to two states with a conserved quantum number are highly correlated. For example for small H_{so} spin is a good quantum number and there will be no matrix elements between two opposite spin states. Thus the degeneracy will be lifted due to the surface roughness except for the twofold spin degeneracy. Further, it was shown by

Efetov that the remaining matrix elements can be treated as uncorrelated in good approximation [24].

Table 3.2.1: overview of different Hamiltonian symmetries with their corresponding name for the probability distribution.

Probability distribution	***Magnetic field***	***Spin-orbit coupling***
Poisson	Large	Small
Orthogonal	Small Small	Small Large (even particles)
Unitary	Large	Large
Sympletic	Small	Large (odd particles)

Above it was explained that within random matrix theory a collection of clusters of equal size can be treated as a collection of random matrices restricted to certain symmetry properties. The energy distribution could then be obtained from diagonalizing these matrices. In the following this is demonstrated for a collection of Hermitian, time-invariant and rotational invariant 2x2 matrices of the form:

$$H = \begin{vmatrix} H_{11} & H_{12} \\ H_{21} & H_{22} \end{vmatrix}. \tag{3.6}$$

From (3.5) it can be seen that the basis of this matrix can be chosen arbitrarily. Time-invariance implies that the matrix elements of H to be real and Hermiticity then gives $H_{21} = H_{12}$. The probability distribution $P(H)$ to find a certain Hamiltonian H in the entire collection is further characterized by the following two properties:

- The elements H_{11}, H_{22} en H_{12} are uncorrelated, resulting in $P(H)=P_{11}(H_{11})P_{22}(H_{22})P_{12}(H_{12})$. This assumption is proved by Efetov [24].
- The probability distribution $P(H)$ is invariant for unitairy transformations of the basis states. This follows from the fact that they can be arbitrarily chosen in (3.5).

To be more precise, in this case the matrix elements are real so that the unitary transformation becomes orthogonal. Such an orthogonal transformation corresponds to the rotation of the basis states. Each rotation can be composed of a sum of infinitesimal rotations. Therefore it suffices to consider infinitesimal transformations like

$$\begin{aligned} |1'\rangle &= |1\rangle + e|2\rangle, \\ |2'\rangle &= -e|1\rangle + |2\rangle. \end{aligned} \tag{3.7}$$

Here e is an infinestimal small number and $|1\rangle$ and $|2\rangle$ are two arbitrarily chosen orthonormal basis states.
With this transformation and using $Hb=Eb \rightarrow HU^{-1}a=EU^{-1}a \rightarrow (UHU^{-1})a=H_{new}a=Ea$, the matrix elements in the new basis are to a first order in e as follows

$$
\begin{aligned}
H_{1'1'} &= H_{11} + 2eH_{12}, \\
H_{1'2'} &= H_{12} + e(H_{22} - H_{11}), \\
H_{2'2'} &= H_{22} - 2eH_{12}.
\end{aligned}
\tag{3.8}
$$

From the invariance of the probability distribution with respect to a transformation of the basis it follows that

$$
P(H) = P(H') = P(H)\left\{1 + e\left[\frac{2H_{12}}{P_{11}}\frac{dP_{11}}{dH_{11}} + \frac{H_{22} - H_{11}}{P_{12}}\frac{dP_{12}}{dH_{12}} - \frac{2H_{12}}{P_{22}}\frac{dP_{22}}{dH_{22}}\right]\right\}. \tag{3.9}
$$

Thus the term between the square brackets has to be equal to zero. This term can be rewritten as

$$
\frac{1}{P_{12}H_{12}}\frac{dP_{12}}{dH_{12}} + \frac{2}{H_{22} - H_{11}}\left(\frac{1}{P_{22}}\frac{dP_{22}}{dH_{22}} - \frac{1}{P_{11}}\frac{dP_{11}}{dH_{11}}\right) = 0. \tag{3.10}
$$

The first term is only dependent on H_{12} and the other term only depends on H_{11} and H_{22}. From this follows that the first term should be equal to a certain constant C and the second term to minus this constant. For the first term this results in

$$
\frac{dP_{12}}{P_{12}} = -CH_{12}dH_{12} \rightarrow P_{12} = \left(\frac{C}{2\pi}\right)^{1/2}\exp\left(-\frac{C}{2}H_{12}^2\right). \tag{3.11}
$$

This constant can be determined at the end from the normalization conditions. For the second term in a similar way the following can be derived:

$$
\frac{2}{P_{11}}\frac{dP_{11}}{dH_{11}} + CH_{11} = \frac{2}{P_{22}}\frac{dP_{22}}{dH_{22}} + CH_{22} = A. \tag{3.12}
$$

Here A is a constant. The effect of this A is to shift the energy scale from its zero point. Therefore A is taken to be zero. Then the following can be derived from (3.12):

$$
\begin{aligned}
P_{11} &= \left(\frac{C}{4\pi}\right)^{1/2}\exp\left(-\frac{C}{4}H_{11}^2\right), \\
P_{22} &= \left(\frac{C}{4\pi}\right)^{1/2}\exp\left(-\frac{C}{4}H_{22}^2\right).
\end{aligned}
\tag{3.13}
$$

Except for the normalization constant C the probability distribution $P(H)$ is thus found. The next step will be to use a change of variables to obtain an energy level probability distribution. For this purpose the eigenvalues and eigenfunctions of the matrix will be

used to characterize itself. The eigenvalues of the matrix can be expressed in terms of its matrix elements as follows

$$\begin{aligned} E_a &= \frac{1}{2}(H_{11}+H_{22})+\frac{1}{2}\left[(H_{11}-H_{22})^2+4H_{12}^2\right]^{1/2}, \\ E_b &= \frac{1}{2}(H_{11}+H_{22})-\frac{1}{2}\left[(H_{11}-H_{22})^2+4H_{12}^2\right]^{1/2}. \end{aligned} \tag{3.14}$$

The eigenfunctions of the matrix can be expressed in the basis states $|1\rangle$ and $|2\rangle$ as

$$\begin{aligned} |a\rangle &= \cos\theta|1\rangle+\sin\theta|2\rangle, \\ |b\rangle &= -\sin\theta|1\rangle+\cos\theta|2\rangle. \end{aligned} \tag{3.15}$$

The angle θ in equation (3.15) is given by

$$\cot\theta = -\frac{1}{2H_{12}}\left(H_{22}-H_{11}-\left[(H_{22}-H_{11})^2+4H_{12}^2\right]^{1/2}\right). \tag{3.16}$$

It is now possible to rewrite the probability distribution *P(H)* in terms of the eigenvalues and angle θ given by (3.14) and (3.16) respectively. For the Gaussian exponent this results in

$$H_{11}^2+2H_{12}^2+H_{22}^2 = E_a^2+E_b^2. \tag{3.17}$$

To evaluate the transformation of the volume element $dH_{11}dH_{12}dH_{22}$, the following Jacobian has to be calculated

$$\frac{\partial(H_{11},H_{12},H_{22})}{\partial(E_a,E_b,\theta)} = \begin{vmatrix} \frac{\partial H_{11}}{\partial E_a} & \frac{\partial H_{12}}{\partial E_a} & \frac{\partial H_{22}}{\partial E_a} \\ \frac{\partial H_{11}}{\partial E_b} & \frac{\partial H_{12}}{\partial E_b} & \frac{\partial H_{22}}{\partial E_b} \\ \frac{\partial H_{11}}{\partial \theta} & \frac{\partial H_{12}}{\partial \theta} & \frac{\partial H_{22}}{\partial \theta} \end{vmatrix}. \tag{3.18}$$

For the calculation of this Jacobian H_{11}, H_{12} and H_{22} are first expressed in terms of E_a, E_b and θ:

$$\begin{aligned} H_{11} &= E_a\cos^2\theta+E_b\sin^2\theta, \\ H_{12} &= (E_a-E_b)\sin\theta\cos\theta, \\ H_{22} &= E_a\sin^2\theta+E_b\cos^2\theta 1 \end{aligned} \tag{3.19}$$

With the Jacobian calculated via (3.18) and (3.19), the following expression for the probability distribution in terms of E_a, E_b and θ is obtained:

$$P(E_a, E_b, \theta) = \frac{1}{2}\left(\frac{C}{2\pi}\right)^{1/2}(E_a - E_b)\exp\left(-\frac{C}{4}(E_a^2 + E_b^2)\right). \tag{3.20}$$

Except for the constant C which has to be determined from the normalization condition, this is the basic expression for the (two)-level distribution. The derivations performed above for the calculation of this distribution can be simply generalized for an NxN-system. Before some words will be dedicated to an NxN-system, an important distribution which can be derived from (3.20) is discussed. This is the probability distribution $P(\Delta E)$, which gives the probability to find two adjacent energy levels separated by ΔE. From (3.20) this distribution can be found as follows:

$$P(\Delta E) = \int P(E_a, E_b, \theta)\delta(\Delta E - E_a + E_b)dE_a dE_b d\theta = \frac{C}{4}\Delta E \exp\left(-\frac{C(\Delta E)^2}{8}\right). \tag{3.21}$$

The constant C can now be related to the average energy level spacing at the Fermi level as

$$\int_0^\infty \Delta E P(\Delta E) d\Delta E = \delta = \left(\frac{2\pi}{C}\right)^{1/2} \rightarrow C = \frac{2\pi}{\delta^2}. \tag{3.22}$$

Thus, the normalized probability distribution reads

$$P(\Delta E) = \frac{\pi}{2\delta^2}\Delta E \exp\left(-\frac{\pi}{4}\frac{(\Delta E)^2}{\delta^2}\right). \tag{3.23}$$

This equation is better known as the Wigner surmise. From this equation it can be seen that the level repulsion due to the surface irregularities is taken into account. Namely, for $\Delta E \rightarrow 0$ the probability distribution approaches zero. Further, this distribution is independent on θ meaning that it does not depend on the chosen basis.

The derivation of the energy level distribution given by (3.20) can be generalized for the other three ensembles given in table 3.2.1. In this report the other ensembles will not be considered, because for the system under investigation a small external magnetic field and weak spin-orbit coupling is assumed, and therefore the orthogonal ensemble is valid.

Equation (3.20) is derived for a collection of 2x2 matrices and from this it is only possible to obtain a probability distribution for nearest neighbors. To go beyond this, a collection of larger matrices should be considered. Therefore, a collection of NxN matrices will be shortly discussed here. Here N is the degeneracy of the Fermi level. For the collection of NxN matrices the derivation of the energy distribution is similar to the

case of 2x2 matrices. The same conditions, that the matrix elements are uncorrelated and the probability distribution is independent on the basis, also characterize this energy distribution. The energy distribution is again found from *P(H)* by using a coordinate transformation. *P(H)* is found by performing the rotation (3.7) successively in each of the *N(N-1)/2* 2x2-subspaces. In such a way it is shown that the off-diagonal matrix elements have the probability distribution given by (3.11) and the diagonal elements that of (3.13). Thus *P(H)* is given by

$$P(H) = 2^{-N/2}\left(\frac{C}{2\pi}\right)^{N(N+1)/4} \exp\left(-\frac{C}{4}Tr\left(H^2\right)\right). \tag{3.24}$$

Here *Tr(…)* is the trace and *C* is a constant. The next step is to use a coordinate transformation from the variables H_{ij} to the *N* eigenvalues E_α and *N(N-1)/2* other variables corresponding to the structure of the *N* eigenfunctions. The exponent of (3.24) becomes

$$Tr\left(H^2\right) = \sum_{\alpha=1}^{N} E_\alpha^2 \,. \tag{3.25}$$

As a last step, the Jacobian must be evaluated. The dependence of the Jacobian on E_α can be obtained from a dimensional argument [25]. Namely, the variables H_{ij} are linear functions of E_α (see (3.19)). Therefore the Jacobian must be a symmetric polynomial of order *N(N-1)/2* in E_α. From this argument the following distribution is obtained:

$$P_N(E_1,...,E_N,\theta_1,...,\theta_v) = s(\theta_1,...,\theta_v)\prod_{\alpha<\beta}\left|E_\alpha - E_\beta\right| \exp\left(-\frac{1}{2}\sum_\alpha E_\alpha^2\right). \tag{3.26}$$

Integrating this distribution over all the variables θ results in

$$P_N(E_1,E_2,.....,E_N) = C_N \exp\left(-\frac{1}{2}\sum_i E_i^2\right)\prod_{j<k}\left|E_j - E_k\right|. \tag{3.27}$$

Here C_N is a constant which again has to be determined from normalization. For the thermodynamic properties of the cluster system only a few energy levels around the Fermi level are important. Therefore equation (3.27) is integrated over all but a few in the middle of the distribution which leads to a distribution of energy levels near the Fermi-energy:

$$P_{n-1}(E_i,....,E_{i+n}) = \lim_{N\to\infty}\int P_N(E_1,E_2,.....,E_N)dE_1...dE_{i-1}dE_{i+n+1}...dE_N \,. \tag{3.28}$$

The limit $N \to \infty$ is considered, because in general there are many levels above and below the Fermi level. Here P_{n-1} is a function of *n* level spacings (the subscript *n-1* denotes the number of levels between the lowest and highest one), because around the

center the absolute position of the levels is irrelevant. From this level spacing distribution, the distribution for two adjacent energy levels can be derived. For small ΔE compared to δ this results in

$$P_0(\Delta E) = \frac{\pi^2}{6}\frac{\Delta E}{\delta^2}. \tag{3.29}$$

This result can be compared with the limiting behavior $\Delta E << \delta$ of (3.23). It thus can be seen that they only differ in a constant factor. Therefore, for the adjacent energy level distribution the results from a collection of NxN and 2x2 matrices do not differ in physical behavior. Further, numerical results for $P_0(\Delta E)$ are known for the whole range of $\Delta E/\delta$. Over this range the main physical behavior is again the same [20].
Particular, the same kind of analogy can be made for the level spacing distribution $P_1(\Delta_1,\Delta_2)$, where $P_1(\Delta_1,\Delta_2)$ is the distribution of three energy levels with relative spacing Δ_1 and Δ_2. In this case it can also be shown that in a good approximation this distribution can be derived from an ensemble of 3x3 matrices, or $N=3$ in equation (3.24), resulting in

$$P_3(\Delta,\Delta') = \Omega_3\delta^{-5}[\Delta\Delta'(\Delta+\Delta')]\exp[-(\Delta^2+\Delta\Delta'+\Delta'^2)/3\delta]^2. \tag{3.30}$$

Here the subscript 3 denotes that it is the relative level distribution of three energy levels and Ω_3 is a constant to be determined from normalization of the distribution.

As a last step the probability function that can be obtained from random matrix theory, $R(|E|)$ is discussed. This is the probability to find two energy levels separated by $|E|$ no matter how many energy levels there are in between them. For the calculation of this probability the following sum has to be evaluated:

$$R(|E|) = \sum_{n=0}^{\infty} P_n(|E|). \tag{3.31}$$

Here $P_n(|E|)$ is the probability to find two energy levels separated by $|E|$ with exactly n levels in between them. This sum was calculated by Dyson who found the following for an orthogonal ensemble [26]:

$$R(|E|) = 1 - \left(\frac{\sin\left(\frac{\pi E}{\delta}\right)}{\frac{\pi E}{\delta}}\right)^2 - \frac{d}{d\left(\frac{E}{\delta}\right)}\left(\frac{\sin\left(\frac{\pi E}{\delta}\right)}{\frac{\pi E}{\delta}}\right)\cdot\int_{\frac{E}{\delta}}^{\infty}\frac{\sin(\pi x)}{\pi x}dx. \tag{3.32}$$

This probability distribution will be used below in paragraph 3.4 to derive the expression for the transverse dynamic magnetic susceptibility for a collection of clusters.

Summarizing, in this paragraph it was shown how within random matrix theory a collection of cluster of the same size, δ, is treated. This resulted in a probability

distribution for the energy level spectrum. From this distribution other useful distributions were derived.

3.3 Calculation of the static magnetic susceptibility and its derivatives

In this paragraph the static magnetic susceptibility is calculated for a non-interacting system (or $f_M(0,0)\big|_{B=0}$). Further, also the first and second derivative of the static susceptibility with respect to the external field (or respectively $\left.\frac{\partial f_M(0,0)}{\partial B}\right|_{B=0}$ and $\left.\frac{\partial^2 f_M(0,0)}{\partial^2 B}\right|_{B=0}$) are calculated. These expressions will be used later in the calculation of equation (2.53).

In the following first the static magnetic susceptibility χ_0 for a non-interacting system is calculated over the whole temperature range. From this result it will become obvious that the static quantities can be calculated as if the bulk limit is still valid. After that the other quantities will be calculated for this bulk limit.

For the calculation of χ_0 over the whole temperature range, the work of Denton et al and Halperin will be followed [2,20]. In the low temperature limit, $k_bT<<\delta$, they calculated the static magnetic susceptibility via the partition sum of which only the most important terms are kept. The justification for the use of the partition sum was already given in the previous paragraph, where it was shown that a cluster can be interpreted as neutral. Further it has been mentioned that there is a difference between odd and even particles. Now first an expression for the static magnetic susceptibility for odd and even particles in the low temperature regime is derived.

The partition sum and the relation between the partition sum and the static magnetic susceptibility are given by

$$Z = 1 + \sum_{j\neq 0} e^{-\beta E_j}, \tag{3.33}$$

$$\chi = \beta^{-1}\frac{\partial^2}{\partial \tilde{H}^2}\ln Z \Rightarrow \chi_0 = \langle\chi\rangle = \beta^{-1}\frac{\partial^2}{\partial \tilde{H}^2}\langle \ln Z\rangle. \tag{3.34}$$

Here Z is the partition sum, χ is the static magnetic susceptibility for a single particle, $\langle\chi\rangle$ is the static magnetic susceptibility for a collection of clusters of the same size and $\beta = (k_B T)^{-1}$. For the evaluation of the partition sum only the first level below and above the Fermi level is taken into account as it is schematically shown in figure 3.3.1. In this figure the possible excitations for the even and odd cases are compared.

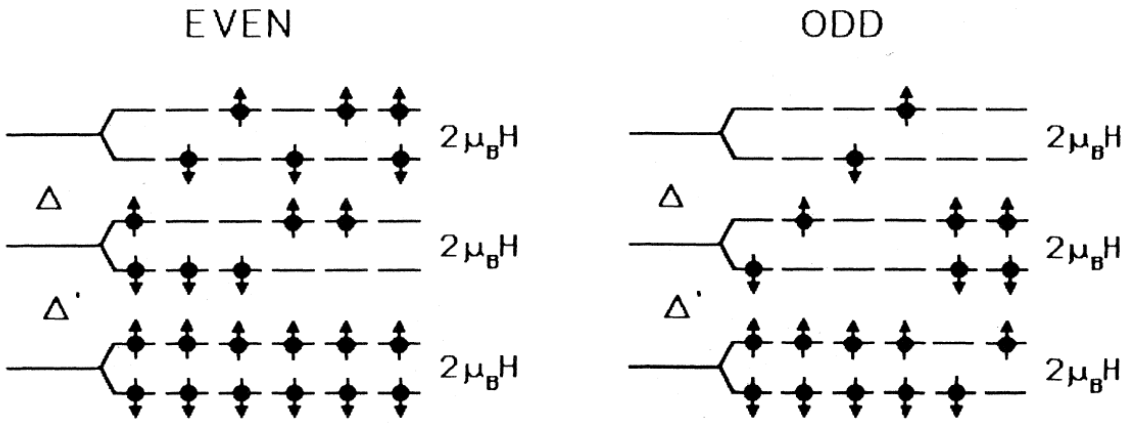

Figure 3.3.1: schematic overview of the excitations around the Fermi level in case of even and odd particles [2].

Writing out the first few excitations of the partition sum explicitly results in

$$\begin{aligned} Z_{even} &= 1+2\left(1+\cosh 2\beta\mu_B\tilde{H}\right)\left(e^{-\beta\Delta}+e^{-\beta(\Delta+\Delta')}+e^{-\beta(2\Delta+\Delta')}\right)+e^{-\beta 2\Delta}+e^{-\beta(2\Delta+\Delta')}, \\ Z_{odd} &= 2\left(\cosh\beta\mu_B\tilde{H}\right)\left(1+e^{-\beta\Delta}+e^{-\beta\Delta'}+3e^{-\beta(\Delta+\Delta')}\right)+e^{-\beta(2\Delta+\Delta')}+e^{-\beta(\Delta+2\Delta')}+e^{-2\beta(\Delta+\Delta')} \\ &+2\left(\cosh\beta\mu_B\tilde{H}\right)e^{-\beta(\Delta+\Delta')}. \end{aligned} \tag{3.35}$$

Considering the most important contributions only, one obtains

$$\begin{aligned} Z_{even} &= 1+2\left(1+\cosh 2\beta\mu_B\tilde{H}\right)\left(e^{-\beta\Delta}\right)+e^{-\beta 2\Delta}, \\ Z_{odd} &= 2\left(\cosh\beta\mu_B\tilde{H}\right)\left(1+e^{-\beta\Delta}+e^{-\beta\Delta'}\right). \end{aligned} \tag{3.36}$$

In case of $\tilde{H}=0$ this gives with the help of (3.34) the following equations

$$\chi^{even} = 2\beta\int P_0(\Delta)(e^{-\beta\Delta})(1+4e^{-\beta\Delta}+e^{-2\beta\Delta})^{-1}\,d\Delta, \tag{3.37}$$

$$\chi^{odd} = \frac{\beta}{4}. \tag{3.38}$$

Here χ^{even} and χ^{odd} are the static magnetic susceptibility in units of $4\mu_b^2$ for an even and odd particle system respectively. For $P_0(\Delta)$ in equation (3.37), the approximate formula of (3.29) can be used. This should hold for sufficient low temperatures, because when Δ becomes of the order of δ then the exponent $e^{-\beta\Delta}$ approaches zero. The result of the averaging with this function is

$$\chi_0^{even} = 1.91 k_b T/\delta^2, \tag{3.39}$$

$$\chi_0^{odd} = \frac{1}{4k_bT}. \tag{3.40}$$

For higher temperatures, $k_bT>>\delta$, it can be expected that there is not much difference between the collection of clusters under investigation and the bulk limit. At high temperatures there are many energy levels involved around the Fermi level and therefore averages like the static susceptibility become insensitive to the exact details of the level distribution. Just as in the bulk case, only the value of the average level spacing around the Fermi level is important. Denton et al uses the equal level spacing approximation in this limit [20]. Also, the general equation for the static magnetic susceptibility given by (2.17) could be used in this regime. Moreover, an interpolation approximation can be used between these two regimes, which will be discussed after the high temperature limit. The result of the high temperature limit was already given in equation (2.18). How this is derived from (2.17) with the use of the Sommerfeld expansion is explained here. For $h \to 0$ equation (2.17) becomes

$$\chi_0 = \int dE \frac{\rho(E)}{2} \cdot \left(-\frac{\partial f}{\partial E} \right). \tag{3.41}$$

The derivative of the Fermi-Dirac function with respect to E deviates substantially from zero only in a region of the order k_bT around the chemical potential $\mu(T)$. In the interesting temperature range $k_bT<<\mu(T)$, and therefore $\rho(E)$ can be Taylor expanded around $\mu(T)$ as

$$\rho(E) = \rho(\mu) + (E-\mu)\frac{d\rho(E)}{dE}\bigg|_{E=\mu} + \frac{1}{2}(E-\mu)^2 \frac{d^2\rho(E)}{d^2E}\bigg|_{E=\mu} + \ldots . \tag{3.42}$$

The first term in this expansion contributes $\rho(\mu)/2$. For the second term one can notice that $\left(-\frac{\partial f}{\partial E} \right)$ is symmetric in $(E-\mu)$ so that all odd powers in the expansion vanish. The second term is calculated as follows:

$$\frac{\rho''(\mu)}{2} \int dE \frac{(E-\mu)^2}{2} \cdot \left(-\frac{\partial f}{\partial E} \right) = (k_bT)^2 \frac{\rho''(\mu)}{2} \int dx \frac{x^2}{2} \cdot \left(-\frac{d}{dx}\left(\frac{1}{e^x+1} \right) \right) =$$

$$(k_bT)^2 \frac{\rho''(\mu)}{2} \frac{\pi^2}{6}. \tag{3.43}$$

Finally, the terms $\rho(\mu)$ and $\rho''(\mu)$ are expanded around E_F as

$$\begin{aligned} \rho(\mu) &= \rho(E_F) + (\mu - E_F)\frac{d\rho(\mu)}{d\mu}\bigg|_{\mu=E_F} + \ldots, \\ \rho''(\mu) &= \rho''(E_F) + (\mu - E_F)\frac{d^3\rho(\mu)}{d^3\mu}\bigg|_{\mu=E_F} + \ldots \end{aligned} \tag{3.44}$$

For μ the following expansion is used which is obtained from the condition that the total number of particles in the system is constant:

$$\mu(T) = E_F - \frac{\pi^2}{12}\frac{(k_b T)^2}{E_F}. \tag{3.45}$$

Then χ_0 up to the second order in k_bT is given by equation (2.18).

Denton et al. developed an approximate interpolation between these two temperature regimes [20]. For this purpose they divided the partition sum in two parts. The first part corresponds to terms with excitation energies E_j smaller or equal to the 'equal level energy' $\overline{E}$ or with other words $E_j \le \overline{E}$. This $\overline{E}$ is found by using the equal level spacing approximation for the energy levels involved in the excitation. Obviously, the second part corresponds to terms with $E_j > \overline{E}$. The n-th order approximation is now given by taking the statistical average over the energy levels which are involved in excitation energies below $\overline{E} = n\delta$. For excitation energies above $n\delta$ the equal level spacing approximation is used even for energy levels lying below $n\delta$. As an example the equation of the first order approximation of the static magnetic susceptibility for an even particle is written out here:

$$\chi_0 = \langle \chi \rangle = \beta^{-1} \int_0^\infty dx_1 P_0(x_1) \left(\frac{\partial^2}{\partial^2 H} \ln\left[Z_{even}(x_1; \beta\delta) \right] \right). \tag{3.46}$$

Here x_1 is the energy spacing between the Fermi level and the nearest level above it. The notation $Z_{even}(x_1;\beta\delta)$ is used to indicate that for excitation energies E_j above δ the adjacent level spacing is put equal to δ. The odd particle case is treated in a similar way, but for the details the reader is referred to [20].
Using lowest order approximations for the even and odd case leads to the results shown in figure 3.3.2. In this figure $\chi_P = \rho(E_F)/2$.

.

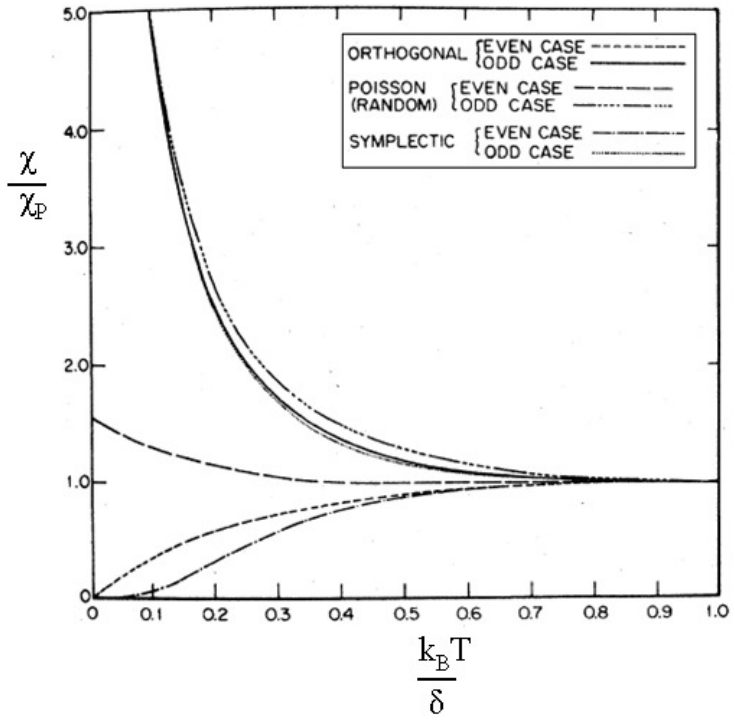

Figure 3.3.2: lowest order interpolations for the even and odd case for different level distributions [20].

From this figure it can be seen that there is fast convergence to the equal level spacing or bulk regime. With other words for $T>\delta$ the static magnetic susceptibility of a cluster system behaves the same as that for bulk. In paragraph 3.5 it will be shown that for the clusters under investigation $T_c>\delta$ and therefore the behavior of the static magnetic susceptibility does not change compared to bulk. Thus in the following the quantities $f_M(0,0)\big|_{B=0}$, $\left.\frac{\partial f_M(0,0)}{\partial B}\right|_{B=0}$ and $\left.\frac{\partial^2 f_M(0,0)}{\partial^2 B}\right|_{B=0}$ will be calculated in the bulk regime.

The first quantity to be evaluated is $f_M(0,0)\big|_{B=0}$. For the paramagnetic phase the magnetization is zero without an external field resulting in

$$f_M(0,0)\big|_{B=0} = f_M(0,0)\big|_{H=0} = \left.\frac{\chi^{-+}_{M0}(0,0)}{\chi^{-+}_{00}(0,0)}\right|_{H=0} = 1\,. \tag{3.47}$$

For the evaluation of the remaining two quantities, they are first rewritten in the following form

$$\left.\frac{\partial f_M(0,0)}{\partial B}\right|_{B=0} = \left.\frac{\partial \chi^{-+}_{M0}(0,0)}{\partial B}\right|_{B=0} \cdot \frac{1}{\chi^{-+}_{00}(0,0)} = \left.\frac{\partial \chi^{-+}_{M0}(0,0)}{\partial H}\right|_{H=0} \cdot \frac{1}{2\mu_b}\frac{1}{\chi^{-+}_{00}(0,0)},$$
$$\left.\frac{\partial^2 f_M(0,0)}{\partial^2 B}\right|_{B=0} = \left.\frac{\partial^2 \chi^{-+}_{M0}(0,0)}{\partial^2 H}\right|_{H=0} \cdot \left(\frac{1}{2\mu_b}\right)^2 \frac{1}{\chi^{-+}_{00}(0,0)}. \qquad (3.48)$$

In this equation a coordinate transformation is used from B to $\tilde{H}$, where $B=2\mu_B\tilde{H}$. The expression for $\chi^{-+}_{00}(0,0)$ is already known, therefore it is left to calculate $\left.\frac{\partial \chi^{-+}_{M0}(0,0)}{\partial H}\right|_{H=0}$ and $\left.\frac{\partial^2 \chi^{-+}_{M0}(0,0)}{\partial^2 H}\right|_{H=0}$. As a starting point for this, equation (2.17) is used which leads for the first term to

$$\left.\frac{\partial \chi^{-+}_{M0}(0,0)}{\partial H}\right|_{H=0} = \mu_b^2 \lim_{H\to 0}\left(\frac{\partial}{\partial H}\int dE \frac{f(E-\mu_b H)-f(E+\mu_b H)}{2\mu_b H}\rho(E)\right) = 0. \qquad (3.49)$$

This means that in the calculation of *G(ω,0)* via equation (2.51), the second term between brackets becomes zero.
For the second term the following is obtained:

$$\left.\frac{\partial^2 \chi^{-+}_{M0}(0,0)}{\partial^2 H}\right|_{H=0} = \mu_b^2 \lim_{H\to 0}\left(\frac{\partial^2}{\partial^2 H}\int dE \frac{f(E-\mu_b H)-f(E+\mu_b H)}{2\mu_b H}\rho(E)\right) = \frac{\mu_b^2}{3}\int dE\rho(E)\left(-\frac{\partial^3 f}{\partial^3 E}\right). \qquad (3.50)$$

To calculate this term, the Sommerfeld expansion is used again. That is, *ρ(E)* is again Taylor expanded around μ. The contribution of the first term, *ρ(μ)*, is zero, because in $\frac{\partial^2 f}{\partial^2 E}$ is zero at minus and plus infinity. For the evaluation of the other terms in this expansion one should note that $\left(-\frac{\partial^3 f}{\partial^3 E}\right)$ is symmetric in *(E-μ)*. The rest of the calculation is similar to the case of χ_0 and the result up to second order in k_BT is

$$\left.\frac{\partial^2 \chi^{-+}_{M0}(0,0)}{\partial^2 H}\right|_{H=0} = \frac{\mu_b^2}{3}\rho''(E_F)\left[1-\frac{\pi^2}{12}\left(\frac{\rho'''(E_F)}{\rho''(E_F)}-2\frac{\rho''''(E_F)}{\rho''(E_F)}\right)(k_bT)^2\right]. \qquad (3.51)$$

The last step is to combine this result with equations (2.18) and (3.48). The resulting expression can also be expanded in terms of k_BT leading to the first term linear in k_BT.

In paragraph 3.5 it will become clear that temperature dependent part of above calculated quantities only leads to unimportant higher order corrections.

Summarizing, for the clusters under investigation it is shown that the static quantities $f_M(0,0)\big|_{B=0}$, $\left.\frac{\partial f_M(0,0)}{\partial B}\right|_{B=0}$, $\left.\frac{\partial^2 f_M(0,0)}{\partial^2 B}\right|_{B=0}$ and χ_0 can be calculated in the bulk limit. From these calculations temperature dependences of these quantities are obtained.

3.4 Calculation of the transverse dynamic magnetic susceptibility

In this paragraph an expression for the dynamic magnetic susceptibility of a non-interacting system will be calculated. For this certain restrictions for ω and q will be used.

As a starting point for the calculation of the transverse dynamic magnetic susceptibility for a non-interacting system, the following expression is used (for the derivation of this term see Appendix):

$$\chi^{-+}_{M0}(\omega,q)=\sum_{\mu'}\sum_{\nu'}\frac{n_{\nu'}-n_{\mu'}}{E_{\nu'}-E_{\mu'}-\omega}\left\langle\mu'\middle|S^-(-q)\middle|\nu'\right\rangle\left\langle\nu'\middle|S^+(q)\middle|\mu'\right\rangle. \tag{3.52}$$

Here $n_{\mu'}$ is the occupation probability of state μ', $E_{\mu'}$ the energy of state μ', $|\mu'\rangle$ is an eigen-state with eigen-value $E_{\mu'}$, $S^-(-q)=e^{-i\vec{q}\cdot\vec{r}}\cdot\sigma_{down}$ and $S^+(q)=e^{i\vec{q}\cdot\vec{r}}\cdot\sigma_{up}$. This σ_{down} and σ_{up} work on spin states and flip the spin state down and up respectively. For the cluster system, it was mentioned in paragraph 3.2 that the particles responsible for the magnetic properties can be interpreted as non-interacting quasi-particles. This means that the occupation probability is a Fermi-Dirac distribution. Further, the energies $E_{\mu'}$ and states $|\mu'\rangle$ then belong to a single quasi-particle state.

Moreover, spin-orbit coupling (H_{so}) was assumed to be very small compared to δ. This means that spin is a good quantum number. Writing out the spin state explicitly in equation (3.52) and executing the spin operators σ, results in

$$\chi^{-+}_{M0}(\omega,q)=\sum_{\mu}\sum_{\nu}\frac{n_{\nu\uparrow}-n_{\mu\downarrow}}{E_{\mu\downarrow}-E_{\nu\uparrow}-\omega}\left\langle\mu\downarrow\middle|e^{-i\vec{q}\cdot\vec{r}}\middle|\nu\downarrow\right\rangle\left\langle\nu\uparrow\middle|e^{i\vec{q}\cdot\vec{r}}\middle|\mu\uparrow\right\rangle=$$
$$\sum_{\mu}\sum_{\nu}\frac{n_{\nu\uparrow}-n_{\mu\downarrow}}{E_{\mu\downarrow}-E_{\nu\uparrow}-\omega}\left|\left\langle\nu\middle|e^{i\vec{q}\cdot\vec{r}}\middle|\mu\right\rangle\right|^2. \tag{3.53}$$

Here the summations over μ and ν do not include the different spin states (spin up or down) anymore. That is, the $|\mu\rangle$ does not contain a spin part while $|\mu'\rangle$ does.

For a non-interacting system the difference between the spin-up and spin-down states can only be caused by a uniform external field $\tilde{H}$. Thus, when using the expression $B(M)=h(M)=2\mu_B\tilde{H}$ equation (3.53) becomes

$$\chi_{M0}^{-+}(\omega,q)=\sum_{\mu}\sum_{\nu}\frac{n(E_\nu-B)-n(E_\mu+B)}{E_\mu-E_\nu+2B-\omega}\left|\left\langle\nu\left|e^{i\vec{q}\cdot\vec{r}}\right|\mu\right\rangle\right|^2 . \tag{3.54}$$

In the rest of the derivation $\tilde{H}$ is set equal to zero, resulting in

$$\chi_{0}^{-+}(\omega,q)=\sum_{\mu}\sum_{\nu}\frac{n(E_\nu)-n(E_\mu)}{E_\mu-E_\nu-\omega}\left|\left\langle\nu\left|e^{i\vec{q}\cdot\vec{r}}\right|\mu\right\rangle\right|^2 . \tag{3.55}$$

In the following the work of Gor'kov and Eliashberg will be used [27]. They calculated the dynamic dielectric susceptibility of a cluster system for small ω.
First equation (3.55) is rewritten as a sum of a static and a dynamic part as follows:

$$\chi_{0}^{-+}(\omega,q)=-\sum_{\nu}\sum_{\mu}\frac{n(E_\nu)-n(E_\mu)}{E_\nu-E_\mu}\left|\left\langle\nu\left|e^{i\vec{q}\cdot\vec{r}}\right|\mu\right\rangle\right|^2 \tag{3.56a}$$

$$-\omega^2\sum_{\mu}\sum_{\nu}\frac{1}{\left(E_\nu-E_\mu\right)^2-\omega^2}\cdot\frac{n(E_\nu)-n(E_\mu)}{E_\nu-E_\mu}\left|\left\langle\nu\left|e^{i\vec{q}\cdot\vec{r}}\right|\mu\right\rangle\right|^2 . \tag{3.56b}$$

For the rest of the derivation equation (3.56b) is called $\overline{\chi}_0^{-+}(\omega,q)$. The next step is to multiply equation (3.56b) with $\frac{R(E_\nu-E_\mu)}{\delta^2}dE_1dE_2$ to obtain an expression for a collection of clusters of the same size. Here $R(E_\mu\text{-}E_\nu)$ is the probability distribution given by (3.32). The result is

$$\overline{\chi}_0^{-+}(\omega,q)=-\frac{\omega^2}{\delta^2}\int_{-\infty}^{\infty}\int_{-\infty}^{\infty}dE_\nu dE_\mu\,\frac{R\left(\left|E_\nu-E_\mu\right|\right)\cdot\left|\left\langle\mu\left|e^{i\vec{q}\cdot\vec{r}}\right|\nu\right\rangle\right|^2}{\left(E_\nu-E_\mu\right)^2-\omega^2}\cdot\frac{n(E_\nu)-n(E_\mu)}{E_\nu-E_\mu}. \tag{3.57}$$

If ω is small as assumed then $\left|\left\langle\mu\left|e^{i\vec{q}\cdot\vec{r}}\right|\nu\right\rangle\right|^2\approx\left|\left\langle\mu\left|e^{i\vec{q}\cdot\vec{r}}\right|\nu\right\rangle\right|^2_{\omega=0}$ is constant [27]. Further, because the integrand diverges at $E_\mu\text{-}E_\nu\sim\omega$, $\frac{n(E_\nu)-n(E_\mu)}{E_\nu-E_\mu}\approx\frac{\partial n(E_\mu)}{\partial E_\mu}$. Thus, equation (3.57) becomes

$$\overline{\chi}_0^{-+}(\omega,q)=\left|\left\langle\mu\left|e^{i\vec{q}\cdot\vec{r}}\right|\nu\right\rangle\right|_0^2\frac{1}{\delta}\frac{A(\omega)}{2}, \tag{3.58}$$

$$A(\omega)=2\frac{\omega^2}{\delta}\int\frac{R(|E|)}{E^2-\omega^2}dE .$$

The term $A(\omega)$ of equation (3.58) can be evaluated by rewriting the term in such a way that the identity of equation (2.25) can be used. This results in

$$A_1(\omega) = 2 - \frac{\sin(2\eta)}{\eta} - 2\eta\left[\int_{\eta}^{\infty} \frac{\cos(t)}{t}\,dt\right]\frac{d}{d\eta}\left(\frac{\sin(\eta)}{\eta}\right), \tag{3.59}$$

$$A_2(\omega) = 2\eta - \frac{2\sin^2(\eta)}{\eta} + 2\eta\left[\int_{0}^{\eta} \frac{\sin(t)}{t}\,dt - \frac{\pi}{2}\right]\frac{d}{d\eta}\left(\frac{\sin(\eta)}{\eta}\right), \tag{3.60}$$

where $A_1(\omega)$ is the real part and $A_2(\omega)$ the imaginary part of $A(\omega)$. Further, $z=2\pi\omega/\delta$ and $\eta=z/2$.To get more insight in these two functions, a plot is made (figure 3.4.1).

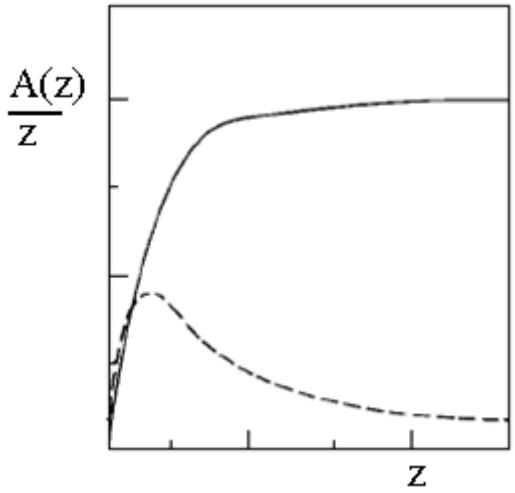

Figure 3.4.1: the dashed line is $A_1(z)/z$ as function of z and the solid line is $A_2(z)/z$ [27].

Thus for small ω, the ω dependence of the dynamic magnetic susceptibility is found. From the considerations below it will appear that z>>1 (*or* $\omega>>\delta$) is the regime of interest. In this regime the real part has much weaker ω dependence than the imaginary part; this is in analogy with the bulk case where the ω dependence is neglected in the real part for small ω and q. This idea will be quantified now. The limiting behavior of $A_1(z)/z$ and $A_2(z)/z$ for $\omega>>\delta$ or $z>>1$ is

$$\frac{A_1(z)}{z} = \frac{2}{z} - \frac{8}{z^3} - 8\frac{\sin(z)}{z^4}, \tag{3.61}$$

$$\frac{A_2(z)}{z} = 1 - \frac{4}{z^2} + \frac{24}{z^4} + 8\frac{\cos(z)}{z^4}. \tag{3.62}$$

It is thus obvious from these two equations that A_2 indeed depends much stronger on ω than A_1.

The justification of the neglect of the ω dependence of the real part compared to that of the imaginary part could also be noticed from figure 3.4.1. Here at $z>1$ $A_1(z)/z$ decreases as $1/z^{\alpha}$ while $A_2(z)/z$ increases.

Thus in the following only the ω dependence in the imaginary part will be taken into account. The next problem is to obtain the q dependence which is in the matrix elements of equation (3.56a) and (3.56b). The exact calculation is tedious and difficult to do. However, there is another simpler approach. In this approach the q dependence in the regime $q_c<<q<<k_F$ is assumed to be similar to that of the bulk case (for $q<<k_F$ or as in (2.54)). In here $q_c \sim 1/R$ with R the diameter of a cluster. This is plausible, because for $q<<q_c$ the wavelength of the perturbation is very large compared to the diameter of the cluster so that the cluster 'sees' only a small part of it. However, for $q>>q_c$ or very small wavelengths compared to cluster dimensions, the particles in the cluster 'see' the same perturbation as the particles in the bulk. Thus for $q_c<<q<<k_F$, the real part of the dynamic magnetic susceptibility has approximately a q^2 dependence and the imaginary part a $1/q$ dependence. This results for small ω and $q_c<<q<<k_F$ in the following approximation for f_0,

$$f_0(\omega, q) = 1 - Aq^2 + iC\frac{\omega}{q}\frac{A_2(z)}{z}. \tag{3.63}$$

Here A and C are constants of equation (2.32). The factor $\omega A_2(z)/z$ is used instead of $A_2(z)$ so that the δ dependence disappears when going to the bulk limit or δ is very small. Otherwise the dynamic magnetic susceptibility of bulk would dependent on volume, which is obviously unphysical. Indeed, the electronic properties of a cube of 1x1x1cm^3 in size are the same as the one of for example 2x2x2cm^3.

To summarize, here the expression for $\chi_0^{-+}(\omega, q)$ or $f_0(\omega, q)$ for small ω and $q_c<<q<<k_F$ is derived. In the following paragraph this expression and the quantities calculated in the previous paragraph will be used to calculate the corrections to the Curie temperature.

3.5 Finite size effects on the Curie temperature of small metallic clusters

In paragraphs 3.3 and 3.4 in principle all ingredients are calculated, which are necessary for the calculation of the Curie temperature for a cluster system. As explained above, the SCR-theory will be used for this calculation. Thus the Curie temperature follows from (2.52),

$$1 - I\chi_0(T_c) + \lambda(T_c) = 0. \tag{3.64}$$

The static susceptibility χ_0 of a cluster system was evaluated in paragraph 3.3 and the result is given by (2.18). From the discussion in paragraph 3.3 it appeared that for the cluster system under investigation χ_0 could be approximated by χ_0 for bulk (given by (2.18)). Thus the second term of (3.64) does not change the behavior of a cluster system compared to bulk. With other words the second term does not change the Curie temperature of a cluster system compared to bulk. Then the difference (if there is any) should come from the evaluation of λ.

To obtain λ, equation (2.53) has to be evaluated first. For this the results of paragraph 3.3 and equation (3.63) of paragraph 3.4 will be used. In the following first λ will be evaluated.

Calculation of λ

From equation (2.56) it can be seen that λ can be split in a temperature-dependent and temperature-independent part. For the calculation of the temperature independent part an expression of Im($G(\omega,0)$) over the whole ω range is required. The expression found for f_M in the previous paragraph is only valid in the small ω regime. What to do with this temperature independent part will be discussed later. First the temperature dependent part is investigated. For this purpose an expression for Im($G(\omega,0)$) has to be found, which is done via equation (2.53),

$$\mathrm{Im}(G(\omega,0)) = -\frac{\alpha}{\chi_0}\mathrm{Im}\left(\sum_q\left[\frac{f_M\left(\frac{\partial^2 f_M}{\partial^2 B}\right)}{1-f_M}+\frac{\left(\frac{\partial f_M}{\partial B}\right)^2}{(1-f_M)^2}\right]_{B=0}\right). \tag{3.65}$$

In this equation the numerator will be approximated by its static long wavelength limit, which was found in paragraph 3.3. Thus with (3.49) the second term between the square brackets disappears, resulting in

$$\mathrm{Im}(G(\omega,0)) = -\frac{\alpha}{\chi_0}\left(\frac{\partial^2 f_M(0,0)}{\partial^2 B}\right)_{B=0}\sum_q \mathrm{Im}\left(\frac{1}{1-f_0}\right). \tag{3.66}$$

It now comes down to the evaluation of the sum over q. For bulk this sum was replaced by an integral. In case of a cluster system one has to be careful with this replacement, because the sum is taken in steps proportional to *1/R*. This means that the sum can be replaced only by an integral when the function, $q^2\,\mathrm{Im}\left(\frac{1}{1-f_0}\right)$, changes gradually over an interval *1/R*. For large enough cluster sizes f_0 can be approximated by (2.54) in the $q_c<<q<<k_F$ regime. Namely, for large enough cluster sizes the ω dependence differs from bulk only in the small ω regime. In figure 3.5.1 the function $q^2\,\mathrm{Im}\left(\frac{1}{1-f_0}\right)$ is plotted for different ω as function of q. This function has a maximum for $q\sim\omega^{1/3}$. Thus the sum can be replaced by an integral when $q\sim\omega^{1/3}>>1/R$. This means that for $q>>q_c$ the sum over q can be replaced by an integral and for f_0 equation (3.63) can be used.

For the remaining part of the sum, the function to sum over is not known and a replacement by an integral is probably not possible. However, when the function to sum over is finite, the contribution of this part of the sum can be neglected for large enough cluster sizes. This is, because its contribution is then proportional to *1/R*.

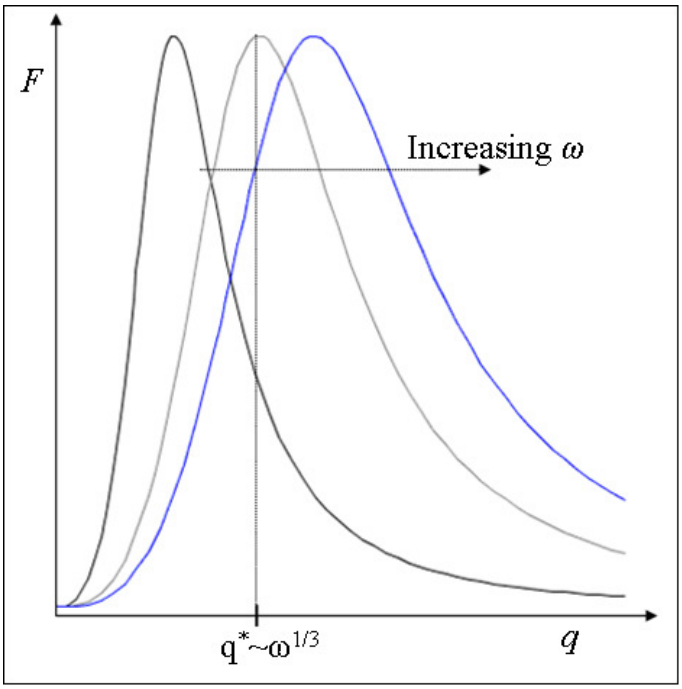

Figure 3.5.1: the function *F*, $q^2\,\mathrm{Im}\left(\frac{1}{1-f_0}\right)$, plotted for different ω as function of *q*.

From the criterion $q>>q_c$ an estimation of the lower limit of the cluster size can be derived. As can be seen from above $q\sim\omega^{1/3}>>1/R$ and with (2.57) can be shown that $q^3\sim\omega\sim T>>1/R^3$. From this the following can be derived,

$$q \sim k_F\left(\frac{T_c}{E_F}\right)^{1/3} \xrightarrow{q>>1/R} (k_F R)^3\,\frac{T_c}{E_F} >> 1 \Rightarrow T_c >> \frac{E_F}{(k_F R)^3} \sim \frac{E_F}{N} \sim \delta. \qquad (3.67)$$

Here δ is the average energy level spacing at the Fermi energy and N was the number of electrons. Estimating E_F by 10^4K and T_c by 20K leads with (3.67) to $N>>500$. Thus, with for example 5 d-electrons per atom this leads to clusters consisting of more than 100 atoms.
Now, from (3.67) it can be understood that in paragraph 3.3 $T>>\delta$ and in paragraph 3.4 $z>>1$ or $\omega>>\delta$ were the regimes of interest.

As discussed above in the calculation of equation (3.66) only the regime $q>>q_c$ of the sum has to be considered. In this regime the sum can be replaced by an integral and for f_0 equation (3.63) can be used. Using these approximations, it is easy to see that

$$\mathrm{Im}\{G(\omega+is,0)\} \sim \omega^{1/3}\left(\frac{A_2(z)}{z}\right)^{1/3} \qquad (3.68)$$

With this, the expression for λ_1 for a collection of clusters of the same size becomes

$$\lambda_1 = \frac{1}{\pi}\int_0^\infty d\omega \cdot \frac{1}{e^{\frac{\omega}{T}}-1} \cdot \mathrm{Im}\big(G(\omega+is,0)\big) \sim \int_0^\infty d\omega \cdot \frac{\omega^{1/3}}{e^{\frac{\omega}{T}}-1} \cdot \left(\frac{A_2(z)}{z}\right)^{1/3} \tag{3.69}$$

For further calculations it is convenient to use the coordinate transformation $x = \frac{\omega}{T}$. Then the full expression for λ_1, called $\lambda_{cluster}$ in the following, becomes

$$\lambda_{cluster} \sim T^{4/3}\int_0^\infty dx \cdot \frac{x^{1/3}}{e^x-1} \cdot \left(1 - \left[\frac{\sin\left(\frac{\pi x T}{\delta}\right)}{\frac{\pi x T}{\delta}}\right]^2 + \left[\int_0^{\frac{\pi x T}{\delta}} \frac{\sin(t)}{t}\,dt - \frac{\pi}{2}\right] \cdot \left(\frac{\cos\left(\frac{\pi x T}{\delta}\right)}{\frac{\pi x T}{\delta}} - \frac{\sin\left(\frac{\pi x T}{\delta}\right)}{\left(\frac{\pi x T}{\delta}\right)^2}\right)\right)^{1/3} \tag{3.70}$$

In the following $\lambda_{cluster}$ will be compared with λ_{bulk}. Above in paragraph 2.5 it was found that $\lambda_{bulk} \sim T^{4/3}\int_0^\infty dx \cdot \frac{x^{1/3}}{e^x-1}$. For comparison $\frac{\lambda_{cluster}}{T^{4/3}}$ as a function of $\frac{T}{\delta}$ together with the constant $\frac{\lambda_{bulk}}{T^{4/3}}$ are plotted in figure 3.5.2.

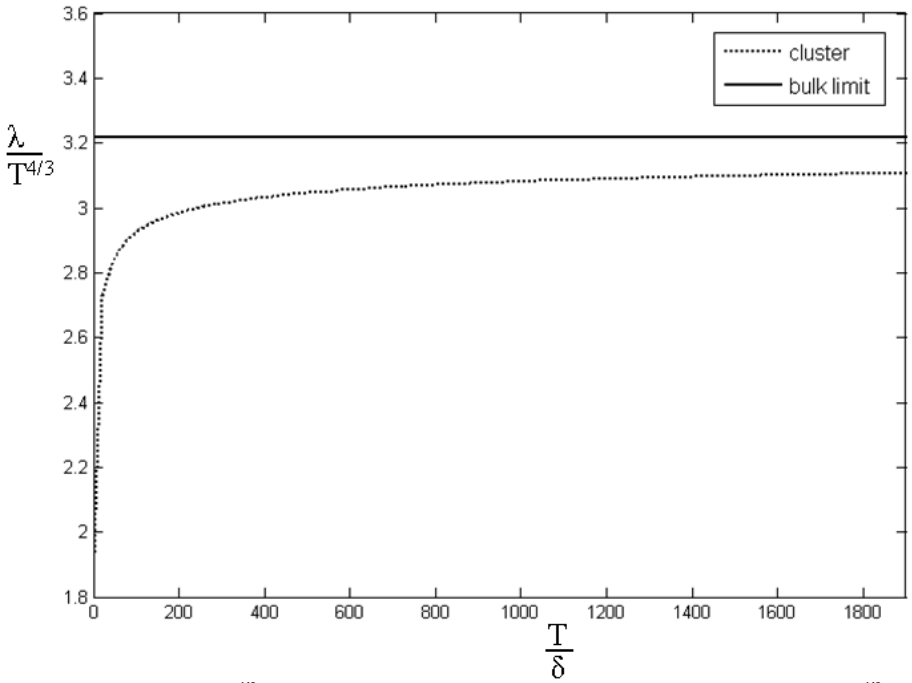

Figure 3.5.2: $\lambda_{cluster}/T^{4/3}$ as a function of T/δ (dotted line) together with $\lambda_{bulk}/T^{4/3}$ (solid line) are plotted.

It can be seen from this figure 3.5.2 that $\lambda_{cluster}$ has a stronger temperature dependence than λ_{bulk} for a fixed size. This means that the Curie temperature of a cluster is increased

compared to bulk. From the figure 3.5.2 it can be seen that this effect increases for smaller cluster sizes. Thus for decreasing cluster sizes the Curie temperature increases. Further, it is also obvious that for very small δ the bulk limit is approached as expected.

Another convenient way to depict the difference between $\lambda_{cluster}$ and λ_{bulk} is to plot both λ_{bulk} and $\lambda_{cluster}$ as a function of temperature in arbitrary units for different values of δ (figure 3.5.3). Obviously this figure could be obtained from the data of figure 3.5.2. However, this is also a convenient way to show the evolution of $\lambda_{cluster}$ with cluster size.

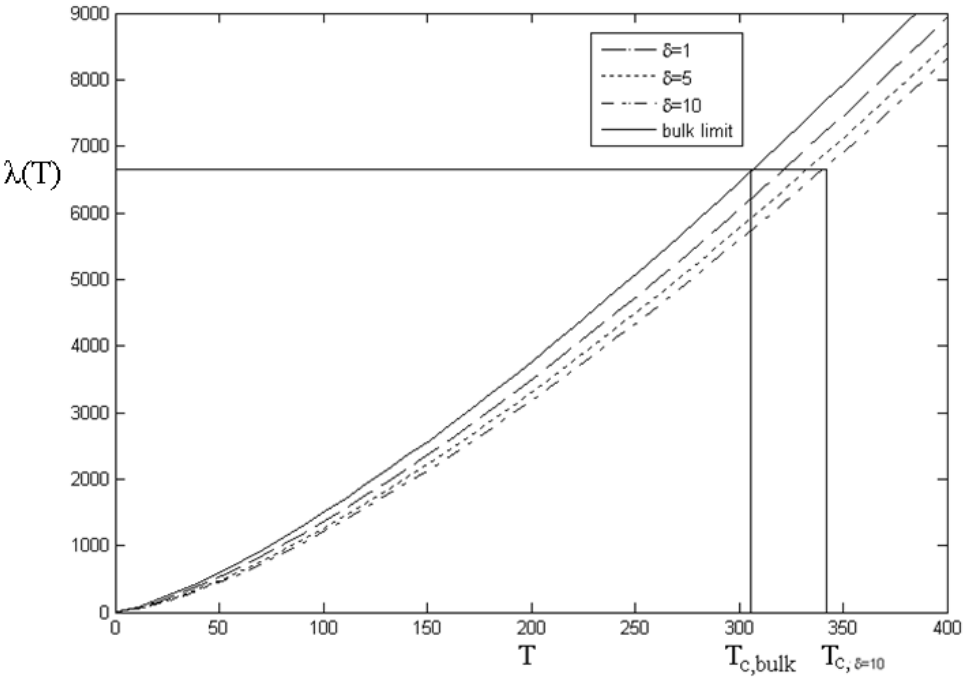

Figure 3.5.3: the solid line is λ_{bulk} as function of temperature. The other lines are $\lambda_{cluster}$ as function of temperature for different values of average distance between neighboring energy levels (δ=1, 5 and 10).

From this figure 3.5.3 there can be clearly seen that the Curie temperature increases for decreasing cluster size. Indeed, let us assume that λ must have a certain value to fulfill (3.64) as indicated by the horizontal line in figure 3.53. Then for the case of bulk a lower Curie temperature is obtained than for the cluster system with $\delta=10$ as indicated by the intersection with the horizontal axis.

From figure 3.5.2 and 3.5.3 it could be seen that the temperature dependence of $\lambda_{cluster}$ differs from λ_{bulk}. For the consideration of equation (3.64) it is important to know that the temperature dependence of $\lambda_{cluster}$ does not exceed the T^2 behavior of χ_0, because then the temperature dependence of $\lambda_{cluster}$ cannot be neglected anymore compared to χ_0. To analyze this point, $\lambda_{cluster}/T^2$ and $\lambda_{cluster}/T^{4/3}$ for certainty are plotted in figure 3.5.4.

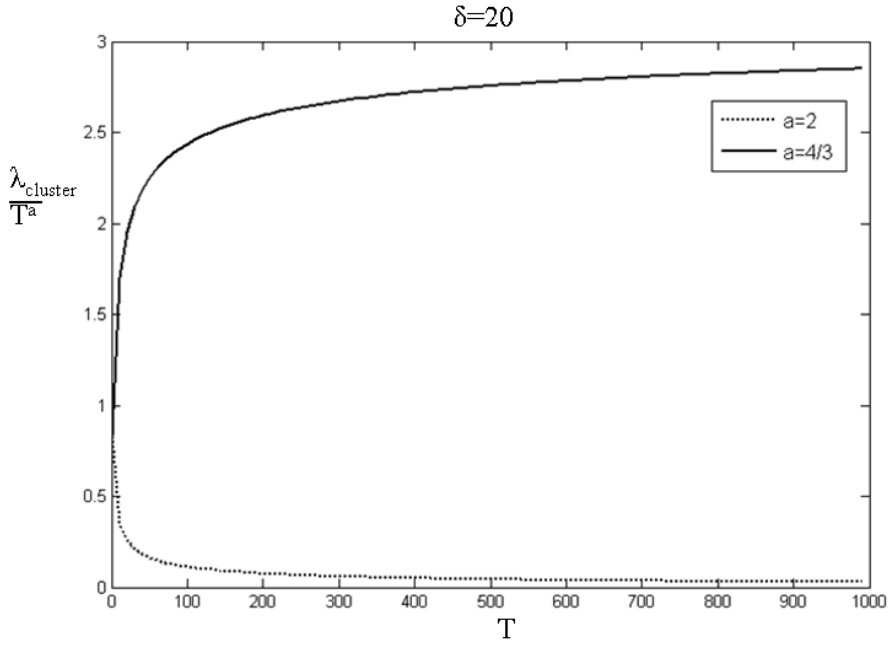

Figure 3.5.4: $\lambda_{cluster}/T^a$ *for a=2 and a=4/3* as function of temperature for δ=*20*.

From this figure it is thus obvious that the temperature dependence of $\lambda_{cluster}$ is weaker than T^2. Thus the temperature dependence of χ_0 can indeed be neglected compared to $\lambda_{cluster}$. From this result it can also be concluded, that the Curie temperature of a cluster system will be below the Curie temperature predicted by the Stoner theory.

Thus from the discussion above it should be obvious that the effect of the temperature dependent part of λ is an increase in Curie temperature for decreasing cluster sizes.

For the calculation of the temperature independent part λ_0 an expression of Im($G(\omega,0)$) over the whole frequency range would be required. This is a tedious calculation and still has to be done. It can be assumed just as for the bulk case that this quantity merrily gives rise to a small shift, which is unimportant compared to the changed temperature dependence in the cluster regime.

Summarizing here, the cluster system under investigation was a collection of similar spherical particles equal in size, but differing in surface roughness. The size of an individual particle was more than roughly 100 atoms. It was also assumed that itinerant electrons were responsible for the magnetic properties and that spin orbit coupling could be neglected. Of this cluster system the Curie temperature was calculated via (3.64). From the work of Denton et al. it could be concluded that χ_0 for clusters does not change compared to bulk. However, the temperature dependence of λ_1 of a cluster system differed from the bulk case giving rise to an increase of the Curie temperature compared to bulk. For smaller cluster sizes this effect increases. The effect of λ_0 still has to be calculated, but probably causes only an important shift.
Thus, by ignoring this λ_0, the main result can be shown best by plotting the Curie temperature of a cluster system as function of size or δ the average level spacing. This is

done in figure 3.5.5, where both the Curie temperature of a cluster system and the average level spacing are normalized to the bulk Curie temperature. In this figure the kink around $\frac{\delta}{T_{c\ bulk}} = 0.02$ arises due to the fact that in this regime to less numerical points were calculated. However, the main result that the Curie temperature of a cluster system increases with decreasing cluster size (increasing δ) is obvious from this figure.

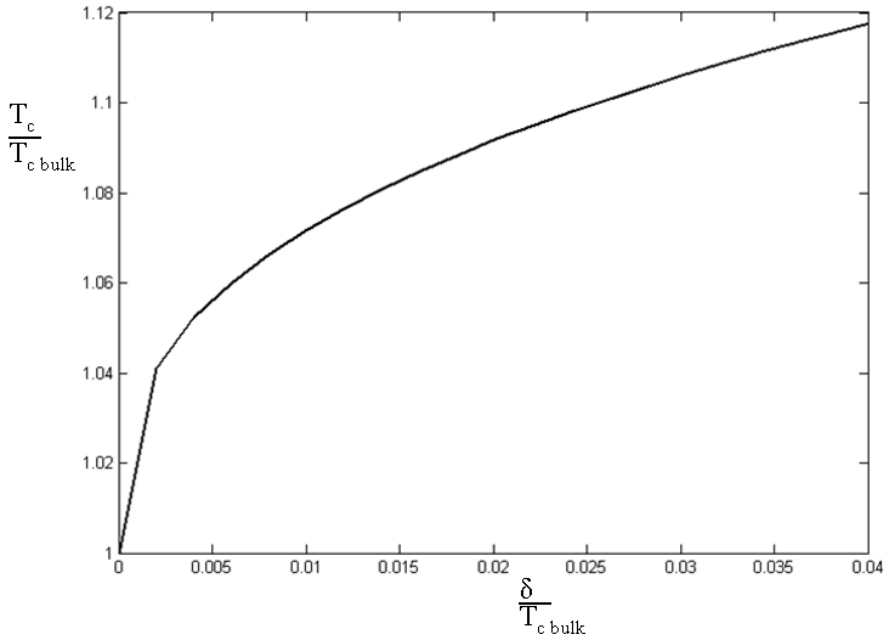

Figure 3.5.5: the Curie temperature of a cluster system normalized to the Curie temperature of the bulk as a function of the average energy level spacing also normalized to the bulk Curie temperature.

Interpretation

Above a quite technical derivation was given of the difference in Curie temperature of a cluster system compared to bulk. In the end the changed temperature dependence of λ_1 caused this difference. This λ term in equation (3.64) can be interpreted as the influence of the spin density fluctuations. Apparently they are suppressed in the cluster system compared to bulk. The mechanism responsible for this must be the mechanism that caused the change in temperature dependence which is the presence of a surface with atomic irregularities. Namely, this surface roughness gives rise to the level repulsion by which the energy level structure changes around the Fermi level. This changed energy level structure on its turn gives rise to a different ω dependence which is via equation (3.70) directly connected to the temperature dependence. Thus due to the presence of an irregular surface spin density fluctuations are suppressed which leads to a higher Curie temperature.

Discussion

For the above described theory, experimental verification is still required. However, there are experimental results on Fe, Ni and Co clusters that could probably be qualitatively understood by the above treated theory [28]. These experimental results show an increase

of the magnetic moment per atomic site for decreasing cluster size. This could be understood as an increase in the Curie temperature for decreasing cluster size caused by the increased suppression of spin density fluctuations for smaller sizes.
The problem is that Fe, Ni and Co are not weakly itinerant electron systems and therefore the above theory cannot be applied. For a correct verification weakly itinerant cluster systems should be prepared and investigated experimentally.

The theory above is appropriate for clusters of approximately larger than 100 atoms. In principle the theory can be extended to smaller cluster sizes. Then χ_0 obtains a different size dependence compared to bulk as shown in paragraph 3.3. Further, the sum over q in equation (2.53) must be evaluated in a different way. Namely, the part neglected in the theory above now becomes important. With other words the discreetness of the spectrum has to be taken into account explicitly.
For even smaller sizes the atomic irregularities become comparable to the size of the cluster and random matrix theory becomes invalid. In this regime a completely different approach has to be used. Mainly ab initio kind of approaches are used in this regime.

Appendix

Here equation (3.52) is derived. As a starting point for this derivation the following expression is used [29]

$$\langle A \rangle = \langle A \rangle_0 + \int_{-\infty}^{\infty} \langle\langle A(t) H_{t'}^1(t') \rangle\rangle dt' . \qquad \text{(A1)}$$

Here $\langle A \rangle$ is the average value of an observable quantity *A*, $\langle A \rangle_0$ is the average of *A* in thermodynamic equilibrium or without a perturbation, $H_{t'}^1(t')$ is a small time dependent perturbation Hamiltonian and $\langle\langle A(t) H_{t'}^1(t') \rangle\rangle = \frac{1}{i\hbar}\theta(t-t')\langle [A(t), H_{t'}^1(t')] \rangle_0$ is the so called two-time retarded Green function.

Equation (A1) describes in linear approximation in $H_{t'}^1$ the retarded response of the average of the observable *A* to the switching on of a perturbation expressed like $H_{t'}^1$ in Hamiltonian form. For the derivation of equation (A1), see [29].

To continue with (A1) it is assumed that the perturbation field is simple harmonic of the form $Re(e^{i\omega t'})$. In general the perturbation term $H_{t'}^1$ can be written as $H_{t'}^1(t') = -\mathrm{Re}\left(\vec{B}(t') \cdot \vec{H}_0 e^{i\omega t'}\right)$, with *B* an observable and H_0 the amplitude of the perturbation field. Thus with this kind of perturbation, the main interest is the Fourier transform of the following Green function

$$G_r(t) = \langle\langle A(t) B(t') \rangle\rangle = \frac{1}{i\hbar}\theta(t-t')\langle [A(t), B(t')] \rangle_0 . \qquad \text{(A2)}$$

Here $G_r(t)$ is the two-time retarded Green function and $\hbar$ is Planck's constant divided by 2π. The Fourier transform of this Green function is

$$G_r(\omega) = \int_{-\infty}^{\infty} G_r(t) e^{i\omega t} dt = \frac{1}{i\hbar} \int_{-\infty}^{\infty} \theta(t-t') \left[\langle A(t) B(t') \rangle_0 - \langle B(t') A(t) \rangle_0 \right] \cdot e^{i\omega(t-t')} dt . \qquad \text{(A3)}$$

The next step is to rewrite the statistical averaged terms like

$$\langle B(t') A(t) \rangle_0 = \sum_l (S_l^* B(t') A(t) S_l) \cdot \langle n_l \rangle = \sum_l \sum_m (S_l^* B(t') S_m)(S_m^* A(t) S_l) \cdot \langle n_l \rangle . \qquad \text{(A4)}$$

Here S_l is a single particle eigenstate, $\langle n_l \rangle$ is the average occupation of state *l* and *(…)* has to be interpreted as an inner product. The expression after the second equality sign is obtained via the closure relation. The statistical averaged terms of (A4) could also be expressed in terms of the eigenstates of the whole system, but it is assumed that in good

approximation the system can be seen as a collection of identical non-interacting quasi-particles. For example the HFA Hubbard model could be used.

Equation (A4) will now be rewritten by using the following equations

$$e^{-\frac{iHt'}{\hbar}} S_l = e^{-\frac{iE_l t'}{\hbar}} S_l, \quad S_m^* e^{\frac{iHt'}{\hbar}} = S_m^* e^{\frac{iE_m t'}{\hbar}} \text{ and} \tag{A5}$$

$$B(t') = e^{\frac{iHt'}{\hbar}} B(0) e^{\frac{-iHt'}{\hbar}} = e^{\frac{iH(t'-t)}{\hbar}} B(t) e^{\frac{-iH(t'-t)}{\hbar}}. \tag{A6}$$

Thus with (A5) and (A6) equation (A4) can be expressed as

$$\begin{aligned} \langle B(t')A(t)\rangle &= \sum_l \sum_m (S_l^* B(t) S_m)(S_m^* A(t) S_l) \cdot \langle n_l \rangle \cdot e^{i\frac{[E_m - E_l](t-t')}{\hbar}} \\ &= \sum_l \sum_m (S_m^* B(t) S_l)(S_l^* A(t) S_m) \cdot \langle n_m \rangle \cdot e^{i\frac{[E_l - E_m](t-t')}{\hbar}}. \end{aligned} \tag{A7}$$

For the term $\langle A(t)B(t')\rangle_0$ a similar derivation can be done which results in

$$\langle A(t)B(t')\rangle_0 = \sum_l \sum_m (S_l^* A(t) S_m)(S_m^* B(t) S_l) \cdot \langle n_l \rangle \cdot e^{i\frac{[E_m - E_l](t-t')}{\hbar}}. \tag{A8}$$

It is convenient for the following derivations to introduce the following function

$$J_{BA}(\omega) = 2\pi \sum_l \sum_m \left(S_m^* B(t) S_l\right)\left(S_l^* A(t) S_m\right) \cdot \langle n_m \rangle \delta\left(\frac{E_m - E_l}{\hbar} - \omega\right). \tag{A9}$$

Here also *(…)* must be interpreted as an inner product. Equations (A7) and (A8) are expressed in terms of $J_{BA}(\omega)$ as follows

$$\langle B(t')A(t)\rangle = \frac{1}{2\pi} \int_{-\infty}^{\infty} J_{BA}(\omega) e^{i\omega(t'-t)} d\omega, \tag{A10}$$

$$\langle A(t)B(t')\rangle = \frac{1}{2\pi} \int_{-\infty}^{\infty} J_{BA}(\omega) \frac{\langle n_l \rangle}{\langle n_m \rangle} e^{i\omega(t'-t)} d\omega. \tag{A11}$$

Substituting equations (A10) and (A11) into (A3) results in

$$G_r(\omega) = \frac{1}{2\pi} \int_{-\infty}^{\infty} d\omega' J_{BA}(\omega') \left[\frac{\langle n_l \rangle}{\langle n_m \rangle} - 1\right] \frac{1}{i\hbar} \int_{-\infty}^{\infty} dt e^{i(\omega-\omega')t} \theta(t). \tag{A12}$$

This expression can be further evaluated by writing the step function as $\theta(t) = \frac{i}{\hbar}\int_{-\infty}^{\infty} \frac{e^{-ixt}}{x+i\varepsilon} dx$. First integrating over *t* and then over *x* gives

$$G_r(\omega) = \frac{1}{2\pi\hbar}\int_{-\infty}^{\infty} d\omega' \frac{J_{BA}(\omega')\left[\frac{\langle n_l \rangle}{\langle n_m \rangle} - 1\right]}{\omega - \omega' + i\varepsilon}. \qquad \text{(A13)}$$

To continue with equation (A13), the expression for $J_{BA}(\omega)$ is substituted into (A13):

$$G_r(\omega) = \frac{1}{2\pi\hbar}\int_{-\infty}^{\infty} d\omega' \cdot 2\pi \frac{\left[\frac{\langle n_l \rangle}{\langle n_m \rangle} - 1\right]\sum_m \sum_l B_{ml} A_{lm} \langle n_m \rangle \delta\left(\frac{E_m - E_l}{\hbar} - \omega'\right)}{\omega - \omega' + i\varepsilon}. \qquad \text{(A14)}$$

Here $B_{ml} = \left(S_m^* B(t) S_l\right)$ and $A_{lm} = \left(S_l^* B(t) S_m\right)$. Integrating (A14) over ω' gives

$$G_r(\omega) = \frac{1}{\hbar}\sum_m \sum_l \frac{B_{ml} A_{lm}\left[\langle n_l \rangle - \langle n_m \rangle\right]}{\frac{E_l - E_m}{\hbar} + \omega + i\varepsilon}. \qquad \text{(A15)}$$

From this equation it is quite easy to obtain (3.52). For this the definition of the transverse dynamic magnetic susceptibility $\frac{\langle S_+(q) \rangle}{h_+(q)}$, $\hbar$ is set to 1 just as in paragraph 2.3 and $H_{t'}^1(t') = -S^+(q)S^-(-q)h_+(q)e^{i\omega t'}$ is used. So *A* of (A15) becomes $S^+(q)$ and *B* becomes $S^-(-q)$.

Literature

[1] J. A. A. J. Peerenboom, P. Wyder and F. Meijer, Electronic Properties of Small Metallic Particles, Phys. Rev. 78, 2 (1981)

[2] W. Halperin, Quantum Size Effects in Metal Particles, Rev. Mod. Phys. 58, 3 (1986)

[3] W. Greiner and Andrey Solov'yov, Atomic cluster physics: new challenges for theory and experiment, Chaos, Solitons and Fractals 25 (2005)

[4] www.teknat.uu.se/forskning/program.php

[5] X. Xu, The Magnetism of Free Cobalt Clusters Measured in Molecular Beams (2007)

[6] P. Langevin, J.Phys. (Paris) 4, 678 (1905); Ann. Chim. Phys. 5, 70 (1905)

[7] T. Moriya, Spin fluctuations in Itinerant Electron Magnetism, Springer-Verlag Berlin Heidelberg New York Tokyo (1985), ISBN 3-540-15422-1

[8] J. Hubbard, Electron Correlations in Narrow Energy Bands, Proc. R. Soc. Lond. A 276 (1963)

[9] P. Fazekas, Lecture Notes on Electron Correlation and Magnetism, World Scientific (1999), ISBN 978-981-02-2474-5

[10] H. Ibach and H. Lüth, Solid State Physics an Introduction to the Principles of Materials Science, Springer, ISBN, 3-540-43870-X

[11] C. Kittel, Introduction to Solid State Physics, ISBN 978-981-02-2474-5

[12] J. O. Dimmock, Solid State Phyiscs 26, 103 (Academic, New York 1971)

[13] O. Gunnarson, J. Phys. F 6, 587 (1976)

[14] B. T. Matthias and R. M. Bozorth, Phys. Rev. 100, 604 (1958)

[15] G. B. Arfken and H. J. Weber, Mathematical Methods for Physicists, Elsevier, ISBN 0-12-088584-0

[16] J. Beille, D. Bloch, M. J. Besnus, J. Phys. F 4, 1275 (1974)

[17] M. Sato, J. Phys. Soc. Jpn. 39, 98 (1975)

[18] T. Moriya and A. Kawabata, Effect of Spin Fluctuations on Itinerant Electron Magnetism, J. Phys. Soc. Jpn. 34, 3 (1972)

[19] T. Moriya and A. Kawabata, Effect of Spin Fluctuations on Itinerant Electron Magnetism II, J. Phys. Soc. Jpn. 35, 3 (1973)

[20] R. Denton, B. Mühlschlegel and D.J. Scalapino, Thermodynamic Properties of Electrons in Small Metal Particles, 1973, Phys. Rev. B 7, 8 (1973)

[21] H. Weyl, Rendiconti del Circulo Matematico di Palermo 39, 1 (1915)

[22] H. Weyl, in Gesammelte Abhandelungen, ed. K. Chaudrasekbaran (Springer Verlag Berlin, 1968) vol. 1 papers 13; 16-19; 22

[23] H. J. Stöckmann, Quantum Chaos: An Introduction, Cambridge University Press, ISBN 0521027152

[24] K. B. Efetov, J. Phys. C 15, L909 (1982a) and K. B. Efetov, Zh. Eksp. Teor. Fiz. 83, 833 [Sov. Phys. JETP 56, 467 (1982)]

[25] A. Bohr and B. Mottelson, Nuclear Structure Volume 1, 1969, (page 294)

[26] F. J. Dyson, J. Math. Phys. 3, 140 (1962)

[27] L. P. Gork'kov and G. M. Eliashberg, Minute Metallic Particles in an Electromagnetic field, 1965, J. Exptl. Theoret. Phys. (U.S.S.R.) 48, 1407-1418

[28] I. M. L. Billas, A. Châtelain and W. A. de Heer, Magnetism from the Atom to the Bulk in Iron, Cobalt, and Nickel Clusters, Science Vol. 265 (1994)

[29] D.N. Zubarev, Non-equilibrium statistical thermodynamics, New York, ISBN 030610895X

[30] E. A. Shapoval, J. Exptl, Theoret. Phys. (U.S.S.R) 47, 1007-1029 (1964)

Acknowledgements

The author of this report would like to thank the following people: Prof. Mikhail Katsnelson, Dr. Andrei Kirilyuk and Prof. Paul Koenraad.
Prof. Mikhail Katsnelson I would like to thank for his support, patience, guidance and above all for answering all the questions I had. Believe me, there were many!
For the help with my presentation and report I want to thank Dr. Andrei Kirilyuk. Further, I would like to thank him for his supervision and help on problems.
As the coordinator from the TUe I would like to thank Prof. Paul Koenraad for his advise and support during the master thesis.